FUNCTIONAL ANALYSES OF MEMBRANE ION CHANNELS: Ca2+ signals by means of fluorescent dyes

Synthetic Fluorescent Ca2+ probes

- These molecular probes specifically bind Ca2+, which causes a change in either the *intensity* or *wavelength of emission* of the probe.
- Changes in concentration of the ion can therefore be monitored.
- There are indicators for most ions, but Ca^{2+} and pH are most commonly used.

- From the chemical point of view, most of the probes are derivatives of the Ca2+ chelators EGTA, and BAPTA

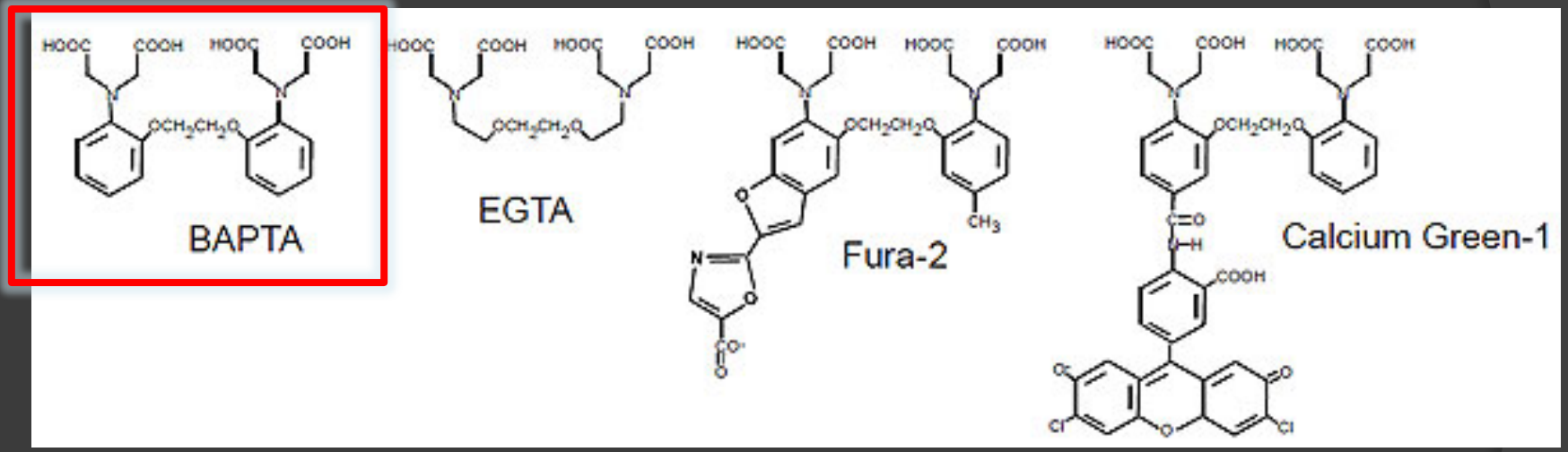

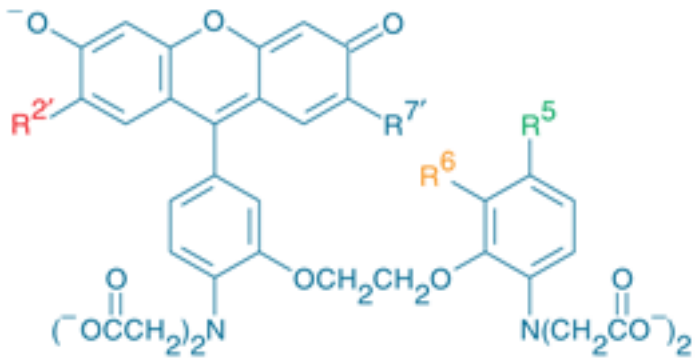

Indicator	$K_d(Ca^{2+})$	$R^{2'}$	$R^{7'}$	R^5	R^6
Fluo-3	0.39 μM	Cl	Cl	CH_3	H
Fluo-4	0.35 μM	F	F	CH_3	H
Fluo-5F	2.3 μM	F	F	F	H
Fluo-5N	90 μM	F	F	NO_2	H
Fluo-4FF	9.7 μM	F	F	F	F

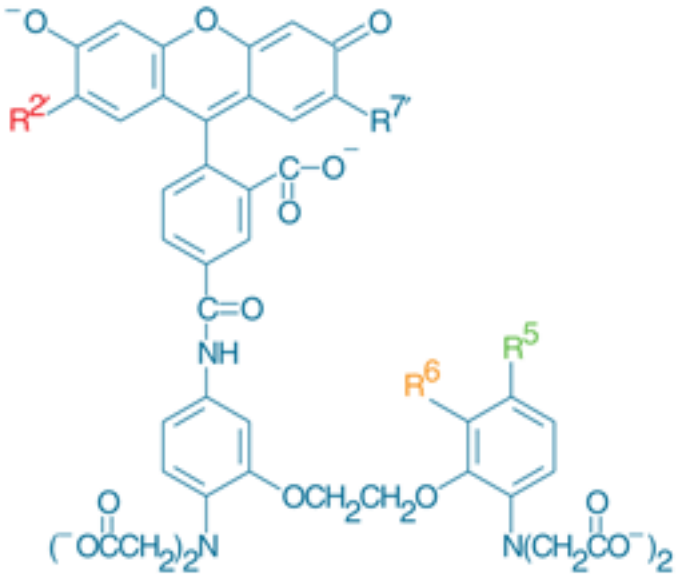

Indicator	$K_d(Ca^{2+})$	$R^{2'}$	$R^{7'}$	R^5	R^6
Calcium Green-1	0.19 μM	Cl	Cl	H	H
Calcium Green-5N	14 μM	Cl	Cl	NO_2	H
Oregon Green 488 BAPTA-1	0.17 μM	F	F	H	H
Oregon Green 488 BAPTA-6F	3 μM	F	F	H	F
Oregon Green 488 BAPTA-5N	20 μM	F	F	NO_2	H

probe incorporation (loading) into the cell

Salt or dextran forms must be microinjected; ester derivatives can be taken up by cells where they are converted to impermeant form. The carboxylate groups of indicators for Ca^{2+} and other cations and the phenolic hydroxyl groups of pH indicators are **derivatized as acetoxymethyl or acetate esters,** respectively, **rendering the indicator permeant to membranes and insensitive to ions**. Once inside the cell, these derivatized indicators are **hydrolyzed by ubiquitous intracellular esterases, releasing the ion-sensitive polyanionic indicator**.

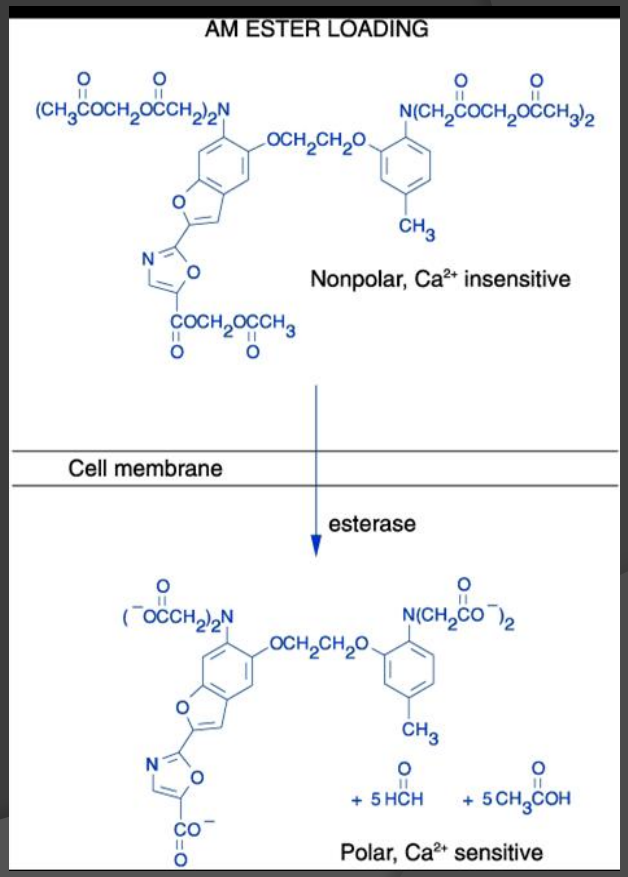

Ca^{2+} Indicators: Fluo-3 has single Ex and Em wavelengths

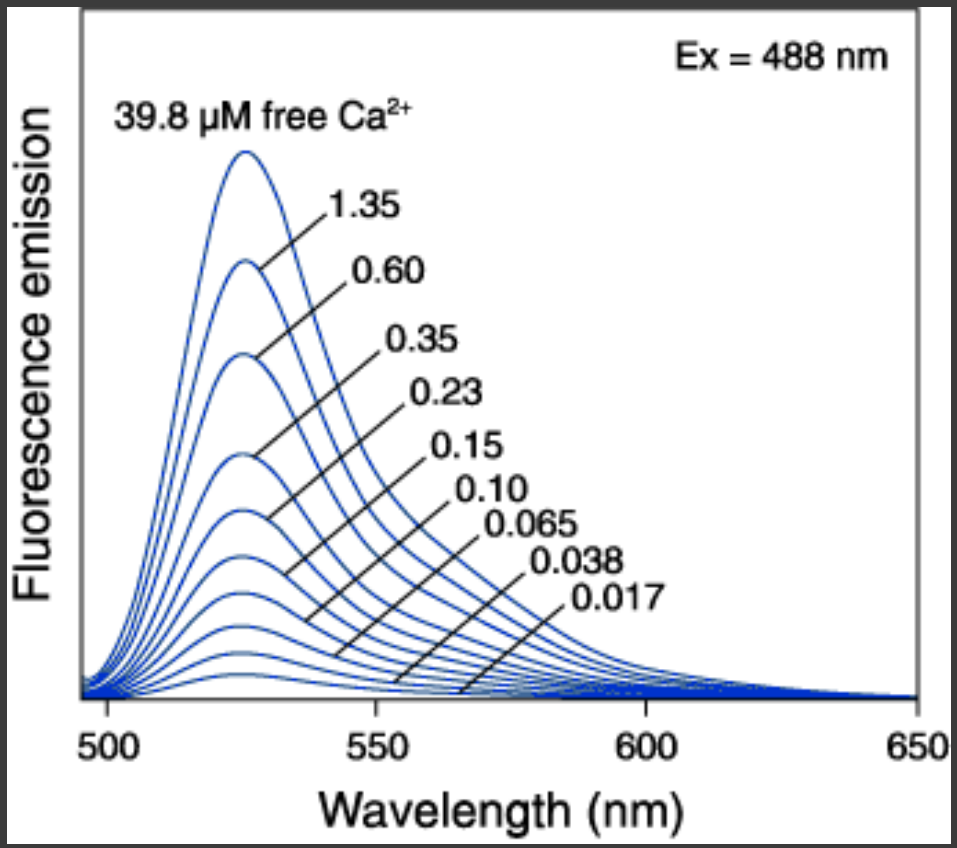

- A visible light excitable dye (488 nm), so Argon laser can be used.
- Emission at 525 nm.
- OK for qualitative detection but not quantitative.

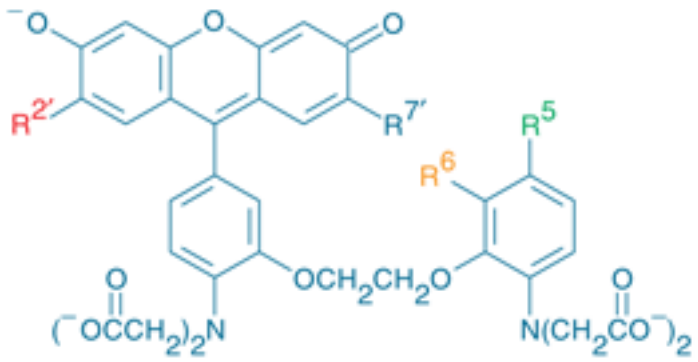

Indicator	$K_d(Ca^{2+})$	$R^{2'}$	$R^{7'}$	R^5	R^6
Fluo-3	0.39 μM	Cl	Cl	CH_3	H
Fluo-4	0.35 μM	F	F	CH_3	H
Fluo-5F	2.3 μM	F	F	F	H
Fluo-5N	90 μM	F	F	NO_2	H
Fluo-4FF	9.7 μM	F	F	F	F

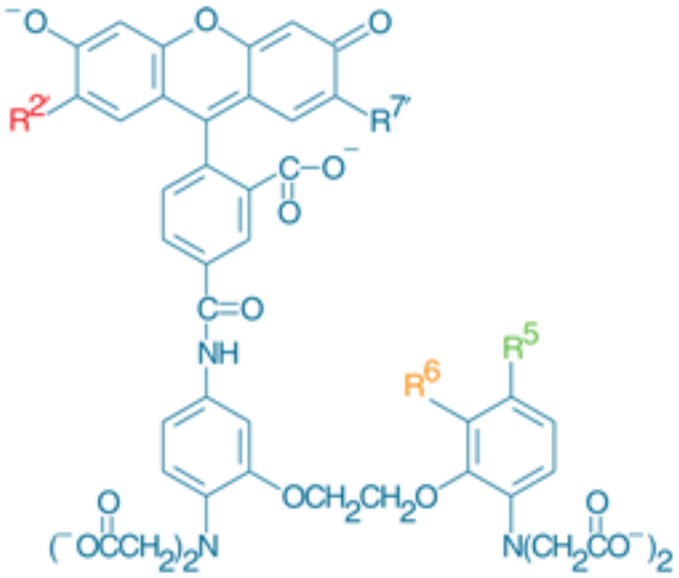

Indicator	$K_d(Ca^{2+})$	$R^{2'}$	$R^{7'}$	R^5	R^6
Calcium Green-1	0.19 μM	Cl	Cl	H	H
Calcium Green-5N	14 μM	Cl	Cl	NO_2	H
Oregon Green 488 BAPTA-1	0.17 μM	F	F	H	H
Oregon Green 488 BAPTA-6F	3 μM	F	F	H	F
Oregon Green 488 BAPTA-5N	20 μM	F	F	NO_2	H

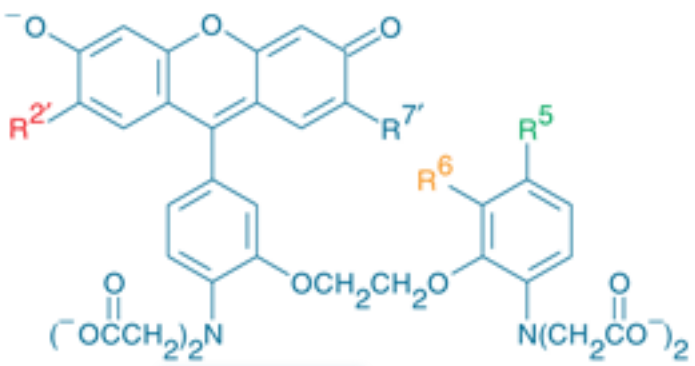

Indicator	$K_d(Ca^{2+})$	$R^{2'}$	$R^{7'}$	R^5	R^6
Fluo-3	0.39 µM	Cl	Cl	CH_3	H
Fluo-4	0.35 µM	F	F	CH_3	H
Fluo-5F	2.3 µM	F	F	F	H
Fluo-5N	90 µM	F	F	NO_2	H
Fluo-4FF	9.7 µM	F	F	F	F

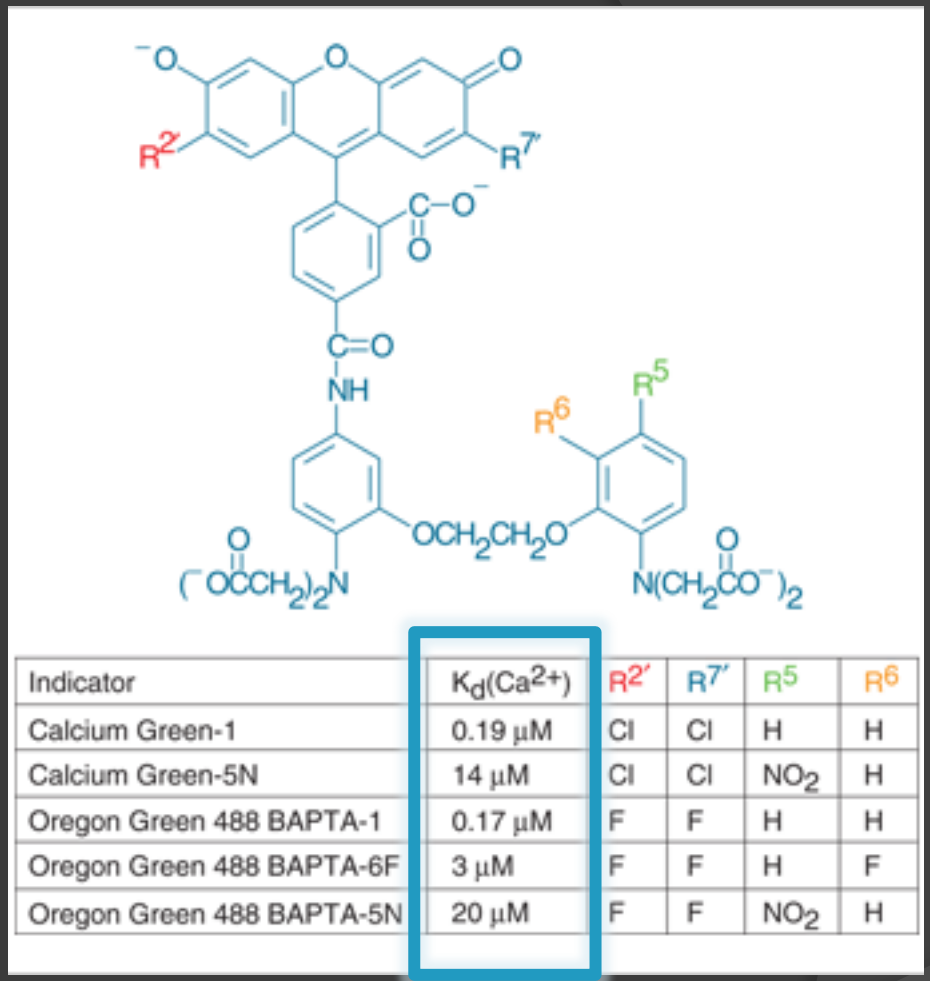

Indicator	$K_d(Ca^{2+})$	$R^{2'}$	$R^{7'}$	R^5	R^6
Calcium Green-1	0.19 µM	Cl	Cl	H	H
Calcium Green-5N	14 µM	Cl	Cl	NO_2	H
Oregon Green 488 BAPTA-1	0.17 µM	F	F	H	H
Oregon Green 488 BAPTA-6F	3 µM	F	F	H	F
Oregon Green 488 BAPTA-5N	20 µM	F	F	NO_2	H

The Kd has molar units and corresponds to the concentration of Ca2+ at which half the indicator molecules are bound with Ca2+ at equilibrium. When possible, indicators should be utilized to measure Ca2+ concentrations between 0.1 and 10 times their Kd. This is the range over which Ca2+ dependent changes in fluorescence are the largest.

UV Ca^{2+} Indicators: Fura-2 is a fixed emission ratiometric dye

Ex at 340 nm and 380 nm

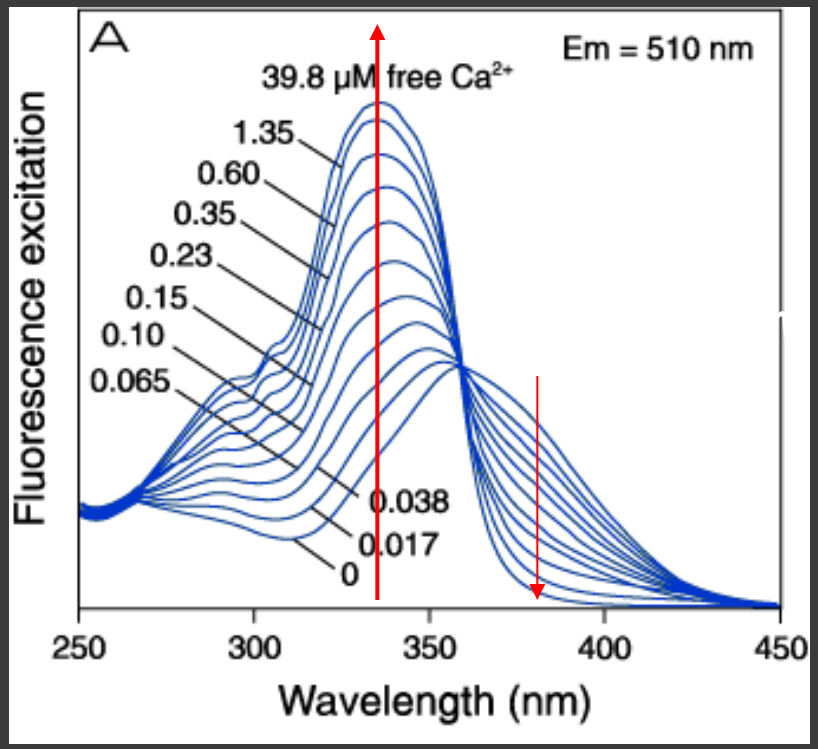

Fura-2

Fura-2 has very limited sensitivity to Ca2+ concentrations above 1 μM. Furthermore, rapid Ca2+ transients monitored by fura-2 photometry are often damped due to the slow rate of Ca2+ dissociation from the indicator. For these reasons, Molecular Probes offers several fura-2 derivatives with lower Ca2+ binding affinity (i.e., higher Kd (Ca2+); Table 1).

UV Ca^{2+} Indicators: Fura-2 is a fixed emission ratiometric dye

Ex at 340 nm and 380 nm

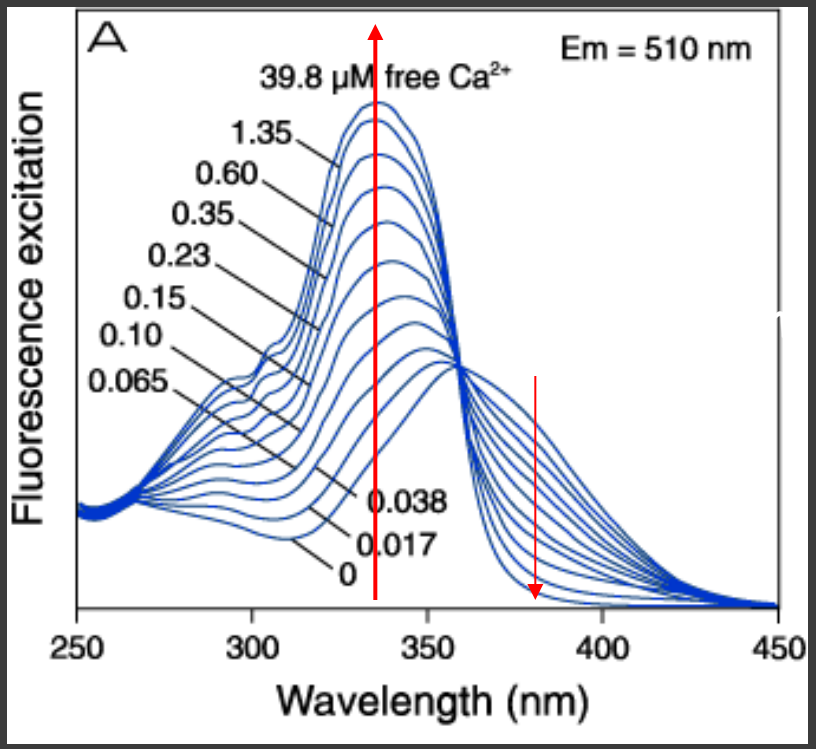

Fura-2

- excitation at 340 and 380 nm. emission at 510 nm
- Ratioing considerably reduces the effects of uneven dye loading, leakage of dye, and photobleaching, as well as problems associated with measuring Ca2+ in cells of unequal thickness.
- In addition, fura-2 and indo-1 are bright enough to permit measurements at intracellular concentrations of dye unlikely to cause significant Ca2+ buffering or damping of Ca2+ transients.

Table 1. Spectroscopic properties and Ca^{2+} dissociation constants for fura-2, indo-1, and their derivatives.

Indicator	Catalog Number		Zero Calcium			High Calcium			K_d (Ca^{2+}) (μM)
	Salt	AM Ester	λ_A † (nm)	ϵ_{max} ‡ ($cm^{-1}M^{-1}$)	λ_F § (nm)	λ_A † (nm)	ϵ_{max} ‡ ($cm^{-1}M^{-1}$)	λ_F § (nm)	
fura-2	F1200, F6799	F1201, F1221, F1225, F14185 *	363	28,000	512 **	335	34,000	505 ††	0.14
bis-fura-2	B6810		366	56,000	511	338	68,000	504	0.37
fura-5F	F14176	F14177	363	26,000	512	336	29,000	506	0.40
fura-4F	F14174	F14175	366	21,000	511	336	23,000	505	0.77
fura-6F	F14178	F14179	364	25,000	512	336	28,000	505	5.30
fura-FF	F14180	F14181	364	25,000	510	335	28,000	506	5.50
indo-1	I1202	I1203, I1223, I1226	346	33,000	475 **	330	33,000	401 ††	0.23
indo-5F	I23912	I23913	344	31,000	471	329	31,000	398	0.47

* High-purity FluoroPure™ grade; † absorption maximum; ‡ molar extinction coefficient; § fluorescence emission maximum; ** fluorescence quantum yield 0.23 for fura-2, 0.38 for indo-1. †† Fluorescence quantum yield 0.49 for fura-2, 0.56 for indo-1. Spectroscopic data and K_d (dissociation constant) values measured in 100 mM KCl, 10 mM MOPS, pH 7.20, 0–10 mM CaEGTA at 22°C.

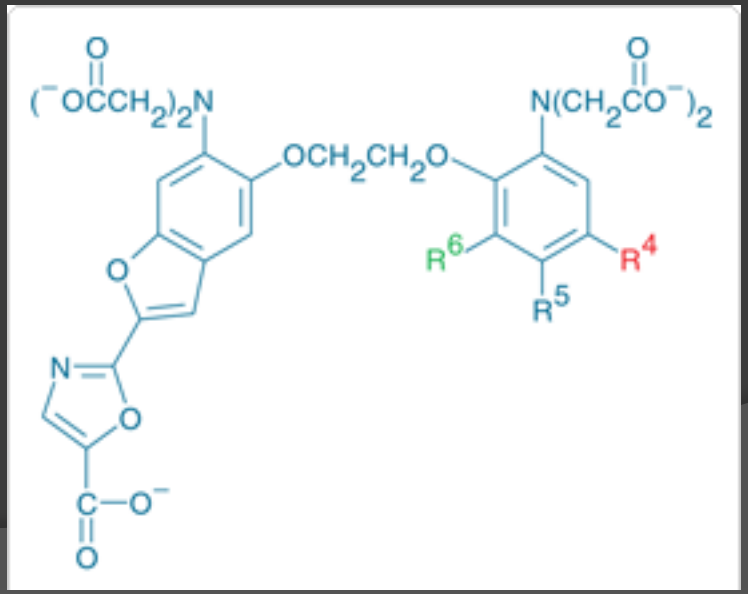

Measurements and Calibration for Fura Indicators

- In contrast to single-wavelength indicators such as fluo-3, the absorption (or fluorescence excitation) maximum of fura indicators shifts from 363 nm for the Ca2+-free chelator to about 335 nm for the Ca2+-bound. The wavelength of maximum fluorescence emission is relatively independent of Ca2+ concentration (Table 1). The largest dynamic range for Ca2+- dependent fluorescence signals is obtained by using ex citation at 340 nm and 380 nm and ratioing the fluorescence intensities detected at ~510 nm. From this ratio, the level of intracellular Ca2+ can be estimated, using dissociation constants (Kd) that are derived from calibration curves.
- By using the *ratio* of fluorescence intensities produced by excitation at two wavelengths factors such as uneven dye distribution and photobleaching are minimized because they should affect both measurements to the same extent.

Measurements and Calibration for Fura Indicators

Once the indicator has been calibrated with solutions of known Ca2+ concentrations, the following equation can be used to relate the intensity ratios to Ca2+ levels:

$$[Ca^{2+}] = K_d \, Q \frac{(R - R_{min})}{(R_{max} - R)}$$

R represents the **fluorescence intensity ratio Fλ1/Fλ2**, in which λ1 (~340 nm) and λ2 (~380 nm) are the fluorescence detection wavelengths for the ion-bound and ion-free indicator, respectively. Ratios corresponding to the titration end points are denoted by the subscripts indicating the minimum and maximum Ca2+ concentration.

Q is the **ratio of Fmin to Fmax at λ2** (~380 nm).

Kd is the **Ca2+ dissociation constant of the indicator**. Calibrating fura indicators requires making measurements for the completely ion-free and ion-saturated indicator (to determine the values for Fmin, Fmax, Rmin, and Rmax) and for the indicator in the presence of known Ca2+ concentrations (to determine Kd).

UV Ca^{2+} Indicators: Indo-1 is a fixed excitation ratiometric dye

Em at 400 nm and 480 nm

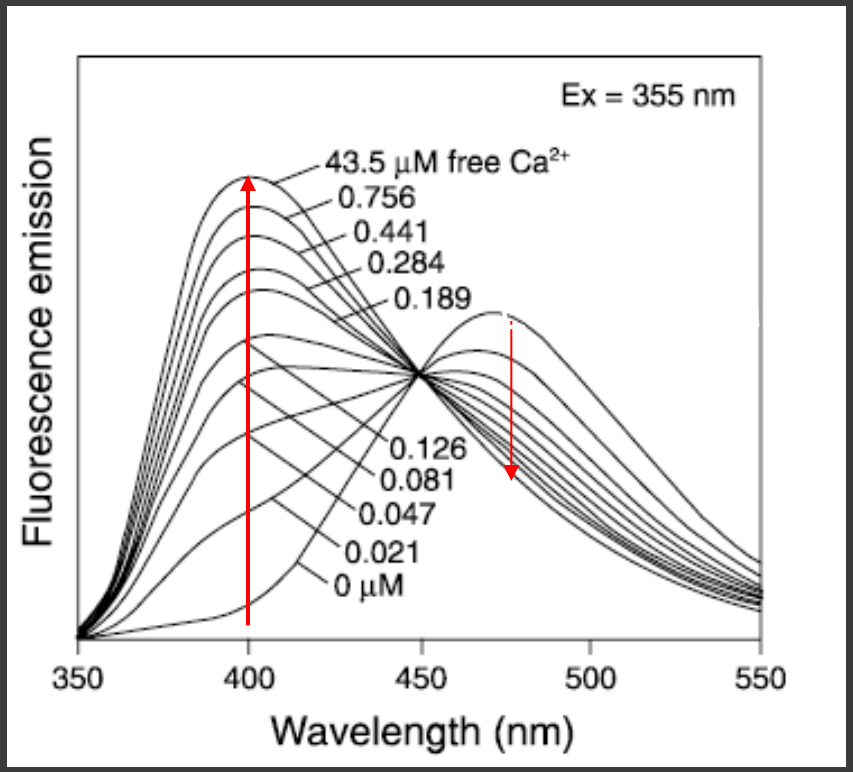

Indo-1

Indo-1 shares most of the advantages of fura indicators except that it is somewhat more light-sensitive. In contrast to fura indicators, which exhibit large changes in absorption on Ca2+ binding, the emission of indo-1 shifts from about 475 nm without Ca2+ to about 400 nm with Ca2+ when excited at about 350 nm.

Equation 1 above may be used for the calibration of indo-1. For this indicator, the value of λ1 is 405 nm while λ2 is 485 nm.

Indo-1 is especially useful for flow cytometry where it is easier to change the emission filters with a single excitation source (often the ultraviolet lines of the argon-ion laser in flow cytometers), and is particularly suited for multicolor fluorescence applications.

Free Ca^{2+} Concentration in a Purkinje Neuron from Embryonic Mouse Cerebellum

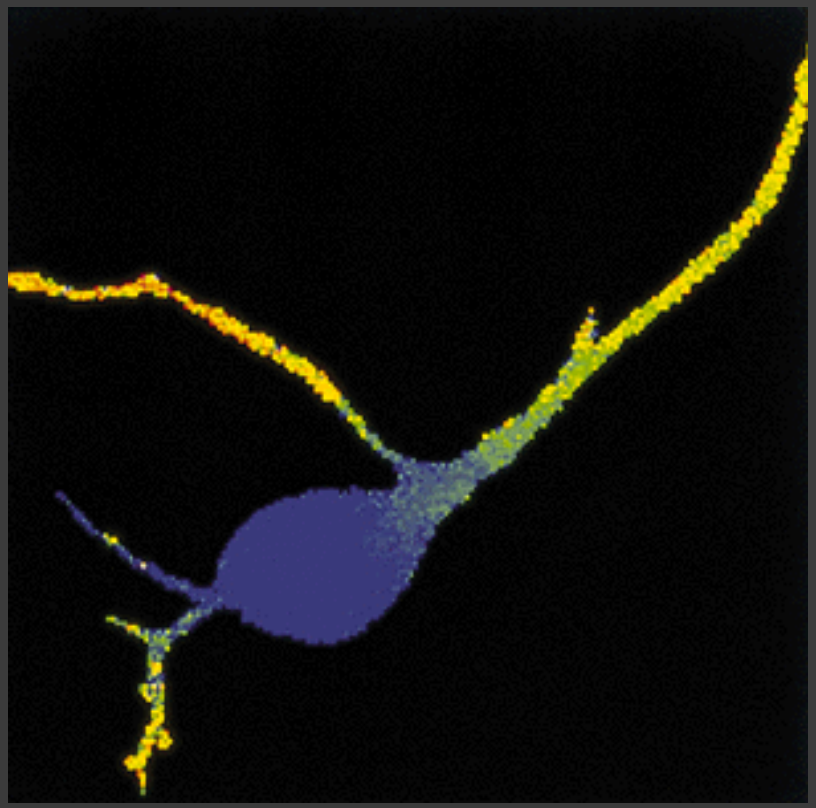

- Neurons were loaded with fura-2.
- Neurons were stimulated with glutamate receptor agonist.
- The composite image represents the ratio of images obtained with excitation at 340 nm and 380 nm.

Dual Blue Ca^{2+} Indicators: Fluo-3 and Fura Red

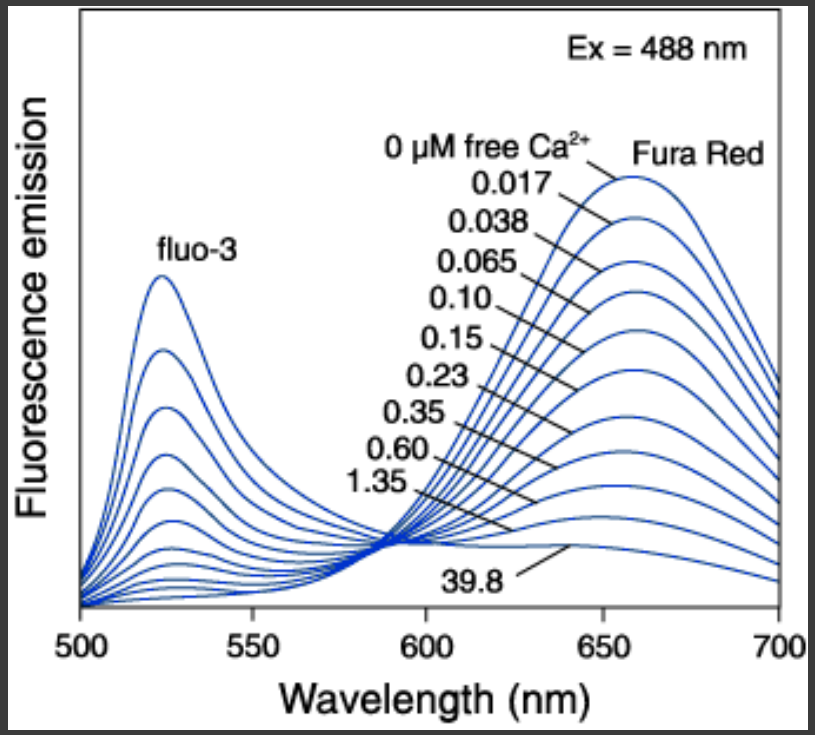

- Use of two dyes solves the problem, e.g. Fluo-3 (increase at 525 with increasing [Ca^{2+}]) and Fura Red (decrease at 650 upon increasing [Ca^{2+}]).
- Both excited by 488 nm.
- [Ca^{2+}] ~ Em of Fluo-3 / Em of Fura Red, independent of [dye].

Genetically encoded Ca2+ indicators (GECI)

intracellular Ca^{2+} detection.

Probe	Origin	Detection technique	Ref.
Aequorin	Genetically encoded	Luminometry	15
Berovin	Genetically encoded	Luminometry	22
Obelin	Genetically encoded	Luminometry	23
Cameleon	Genetically encoded	FRET microscopy	24
Troponin C biosensor	Genetically encoded	FRET microscopy	25
Camgaroo	Genetically encoded	Fluorescence microscopy	26
Ratiometric Pericam	Genetically encoded	Ratiometric fluorescence microscopy	27
GEM-GECO1	Genetically encoded	Ratiometric fluorescence microscopy	28
Calcium Green-1	Synthetic	Fluorescence microscopy	29
Fluo-3, Fluo-4	Synthetic	Fluorescence microscopy	29
Fura-2, Indo-1	Synthetic	Ratiometric fluorescence microscopy	30

Bonora M. et al., 2013 *Nature Proocols*

Genetically encoded Ca2+ indicators (GECI)

intracellular Ca^{2+} detection.

Probe	Origin	Detection technique	Ref.
Aequorin	Genetically encoded	Luminometry	15
Berovin	Genetically encoded	Luminometry	22
Obelin	Genetically encoded	Luminometry	23
Cameleon	Genetically encoded	FRET microscopy	24
Troponin C biosensor	Genetically encoded	FRET microscopy	25
Camgaroo	Genetically encoded	Fluorescence microscopy	26
Ratiometric Pericam	Genetically encoded	Ratiometric fluorescence microscopy	27
GEM-GECO1	Genetically encoded	Ratiometric fluorescence microscopy	28
Calcium Green-1	Synthetic	Fluorescence microscopy	29
Fluo-3, Fluo-4	Synthetic	Fluorescence microscopy	29
Fura-2, Indo-1	Synthetic	Ratiometric fluorescence microscopy	30

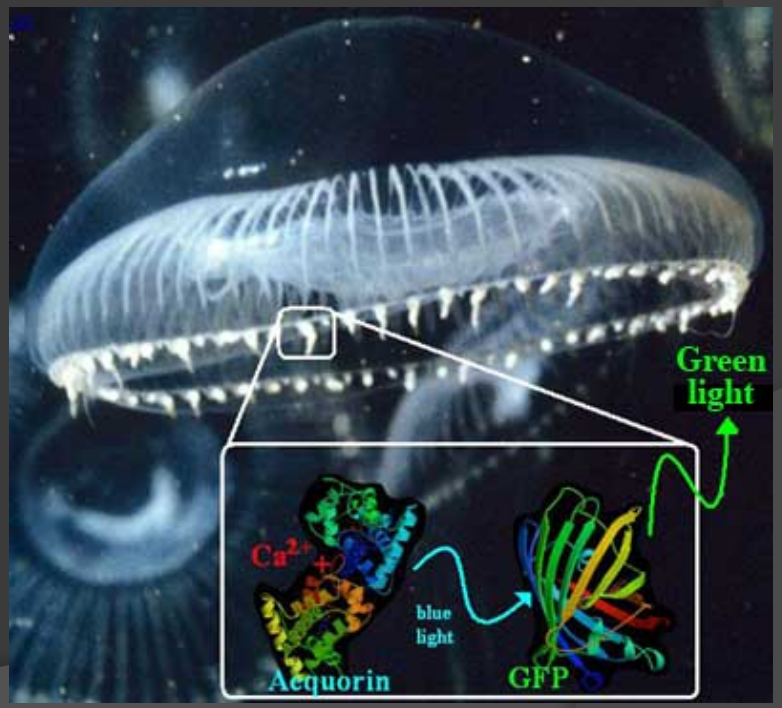

Bonora M. et al., 2013 *Nature Protocols*

AEQUORIN

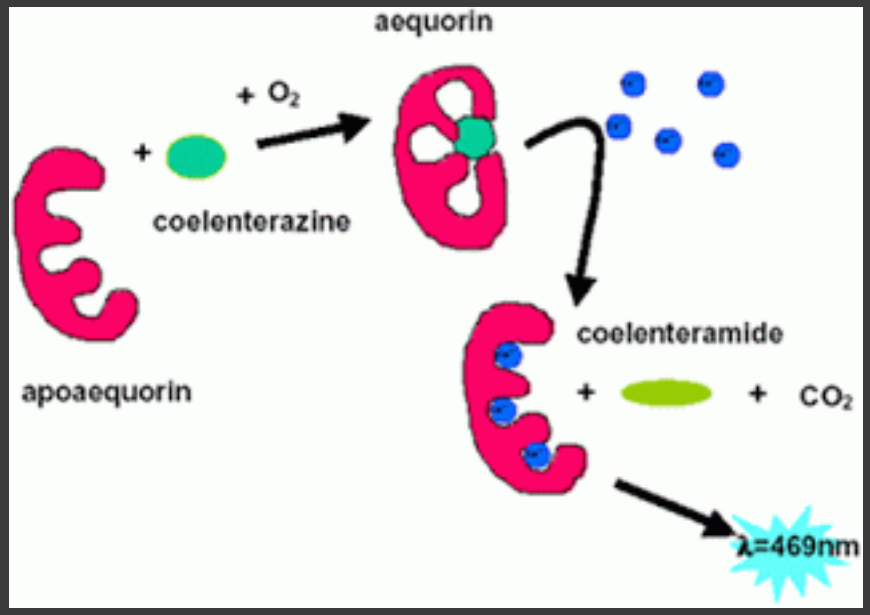

22-kDa protein has had a major role in the study of Ca2+ signaling. Upon binding of Ca2+ to three high-affinity sites, aequorin undergoes an irreversible reaction in which a photon is emitted. In its active form, the protein includes a prosthetic group (coelenterazine) that is oxidized and released in the Ca2+-triggered reaction.

AEQUORIN

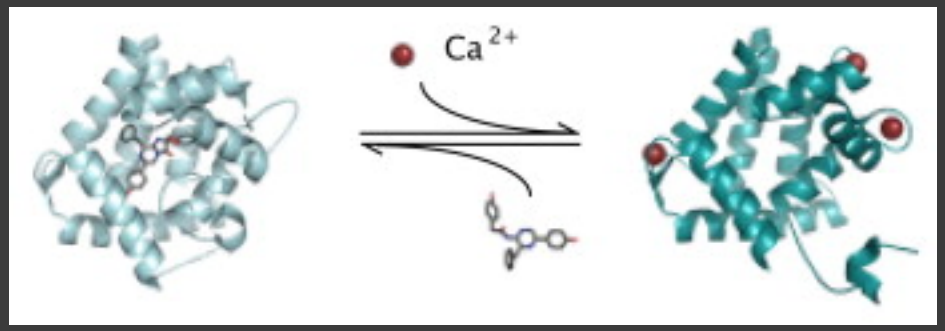
Ca 2+

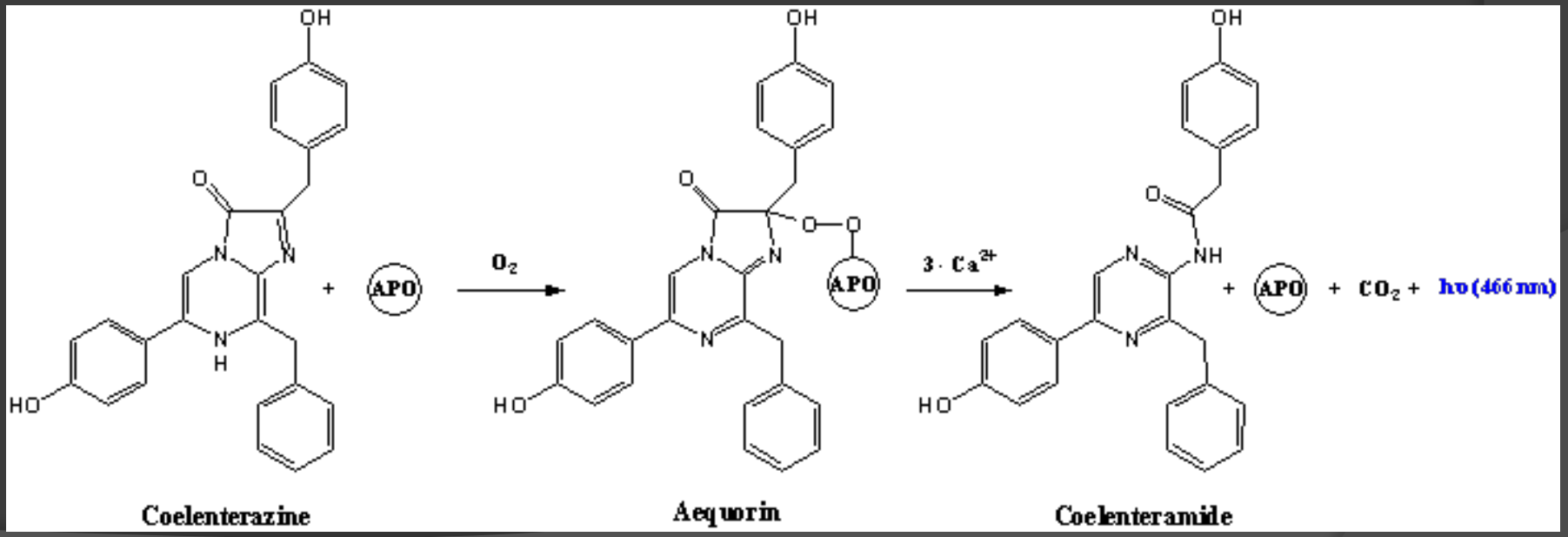
OH
O
N
N
H
HO
+
APO
O2
O—O
3 · Ca2+
NH
+ CO2 +
hυ (466 nm)
Coelenterazine
Aequorin
Coelenteramide

AEQUORIN

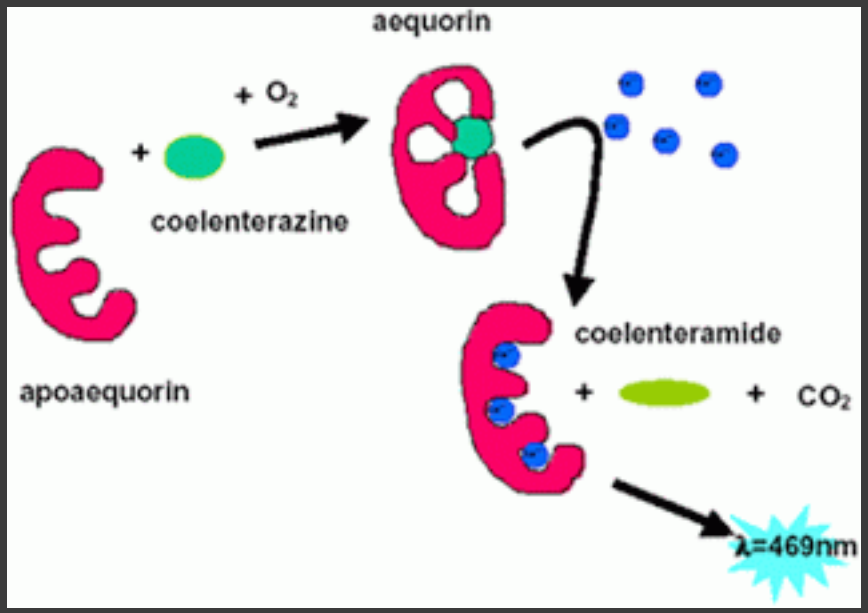

Thus, the expression of aequorin cDNA yields the polypeptide, to which the prosthetic group must be added. Coelenterazine is highly hydrophobic and, when added to the culture medium of aequorin-expressing cells, will freely permeate through the cell membrane. Once inside the cell, coelenterazine spontaneously binds to aequorin, generating the active probe. This procedure is generally termed ‘reconstitution’.

AEQUORIN

There is a relationship between the fractional rate of consumption (i.e., *L*/*L*max, where *L*max is the maximal rate of discharge at saturating Ca2+ concentrations) and [Ca2+].

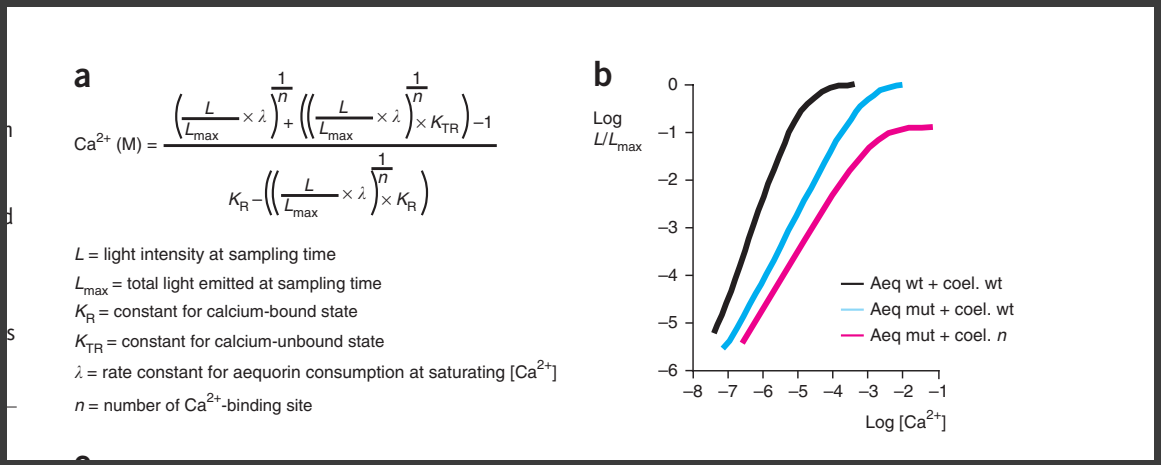

Owing to cooperation between the three binding sites, light emission is proportional to the second to third power of [Ca2+]; this property on the one hand accounts for the **excellent signal-to-noise ratio of aequorin** and on the other hand may subtantially affect the measurements.

AEQUORIN

Given that the probe (differently from fluorescent indicators) is gradually consumed throughout the experiment, the signal tends to decrease, and the conversion into [Ca2+] concentration can be obtained only at the end of the experiment, when, after cell lysis, the total aequorin content is estimated and L/L_{max} can be back calculated for each data point.

Major advantages of using aequorin

Selective intracellular distribution.

The main reason for the renewed interest in using aequorin is that, being a protein, it can be engineered to induce its specific localization to a cell region of interest. Although wild-type aequorin is exclusively cytosolic (cytAEQ), the addition of specific targeting sequences permits selective localization of the photoprotein, resulting in recombinant aequorin chimeras for different intracellular compartments: nucleus (nuAEQ), mitochondria (mtAEQ and mimsAEQ), subplasma-membrane cytosol (pmAEQ), endoplasmic/sarcoplasmic reticulum (erAEQ/srAEQ), Golgi apparatus (goAEQ), secretory vesicles (vampAEQ) and peroxisomes (peroxAEQ).

TABLE 2 | Description of the compartment-specific aequorin chimeras available.

Intracellular localization	Acronym	Targeting strategy
Cytosol	CytAEQ	No targeting sequence is added to aequorin; the sequence of aequorin was modified only by adding the epitope tag HA1 (ref. 15)
Nucleus	NuAEQ	A fragment of rat glucocorticoid receptor, lacking the hormone-binding domain and the nuclear localization signal are fused with the HA1-tagged aequorin[31]
	MtAEQwt	Mitochondrial pre-sequence of subunit VIII of cytocrome *c* oxidase (COX) is fused to the HA1-tagged aequorin, for measurements of $[Ca^{2+}]$ up to 10–15 μM (ref. 32)
Mitochondrial matrix	mtAEQmut	The mutated version of mtAEQwt. Because of the cooperativity between the three Ca^{2+}-binding sites of aequorin, the point mutation (Asp119Ala)[13] that affects the second EF-hand domain, produces a mutated aequorin, which can be used to measure $[Ca^{2+}]$ in the range of 10–500 μM (ref. 33)
	mtAEQmut28,119	Double-mutated form (Asp119Ala and Asn28Leu) of mtAEQwt, which can be used to measure $[Ca^{2+}]$ in the millimolar range for long periods of time, without problems derived from aequorin consumption[14]
Mitochondrial intermembrane space	MimsAEQ	HA1-tagged aequorin is fused (sequence in frame) with glycerol phosphate dehydrogenase, an integral protein of the inner mitochondrial membrane, with a large C-terminal tail protruding on the outer side of the membrane, i.e., in the mitochondrial intermembrane space[34]
Plasma membrane	pmAEQ	The targeting of aequorin to the subplasmalemmal space was based on the construction of a fusion protein including the HA1-tagged aequorin and SNAP-25, a protein that is synthesized on free ribosomes and recruited to the inner surface of the plasma membrane after the palmitoylation of specific cysteine residues[35]
Endoplasmic reticulum	erAEQmut	The encoded polypeptide includes the leader sequence (L), the VDJ and CH1 domains of an Igg2b heavy chain (HC) and the HA1-tagged aequorin at the C-terminus. In this chimera, retention in the ER depends on the presence of the CH1 domain at the N terminus of aequorin. This domain is known to interact with the luminal ER protein BiP, thus causing the retention of the Igg2b HC in the lumen. In the absence of the immunoglobulin light chain, the polypeptide is retained in this compartment[36]
Sarcoplasmic reticulum	srAEQmut	Calsequestrin (CSQ), a resident protein of the sarcoplasmic reticulum, is fused to HA1-tagged aequorin. This chimera is used to measure $[Ca^{2+}]$ in the sarcoplasmic reticulum, the specialized muscle compartment involved in the regulation of Ca^{2+} homeostasis[37]
Golgi apparatus	goAEQmut	Fusion of the HA1-tagged aequorin and the transmembrane portion of sialyltransferase, a resident protein of the Golgi lumen[18]
Secretory vescicles	vampAEQmut	Mutated AEQ (AEQmut; Asp119Ala) is fused to the vesicle-associated membrane protein (vamp)2/synaptobrevin (a vesicle-specific SNARE with a single transmembrane-spanning region) allowing intravesicular $[Ca^{2+}]$ to be monitored[38]
Peroxisomes	peroxAEQ	HA1-tagged wild-type and Asp119Ala mutant aequorins were fused with a peroxisomal targeting sequence[17]

Major advantages of using aequorin

Wide dynamic range.

Native aequorin and its mutants (**Table 2**), in association with different prosthetic groups, are well suited for measuring [Ca2+] from as low as 0.1 μM and up into the mM range.
Numerous chemical modifications of the prosthetic group have been made, which modify, in different ways, the Ca-triggered reaction of the photoprotein. Among these, particularly useful have been those that result in lower light emission at high [Ca2+].
In parallel, single point mutations have been inserted in aequorin cDNAs to reduce its affinity and to allow measurements at higher Ca2+ concentrations. Combinations of mutant aequorins and modified coelenterazine have been used to further increase the dynamic range, allowing measurements in compartments with low [Ca2+] (i.e., cytoplasm or mitochondria in certain cell types), high [Ca2+] (i.e., peroxisomes or mitochondria of other cell) or very high [Ca2+] (i.e., Golgi or ER).

Major advantages of using aequorin

High signal-to-noise ratio.

Mammalian cells are not endowed with chemiluminescent proteins, and thus the background of aequorin measurement is very low. Moreover, the steep relationship between the increases in light emission and Ca2+ concentration accounts for the very large luminescence peaks observed upon stimulation of cells (>1,000–10,000-fold over background can be detected with cytosolic and mitochondrial aequorin, respectively). Because of the excellent signal-to-noise ratio, reliable aequorin measurements can be obtained with moderate levels of expression of the probe.

Major advantages of using aequorin

Low Ca2+-buffering effect.

Aequorin displays an extremely low buffering effect on intracellular Ca2+, negligible if compared with that of fluorescent Ca2+ indicators.

Thus, although in principle, all Ca2+ probes perturb Ca2+ homeostasis because they bind Ca2+ and thus act as Ca2+ buffers, this effect is much less relevant for aequorin than for trappable fluorescent dyes.

As an example, Fura-2 measurements in the presence or absence of aequorin display the same cytoplasmic Ca2+ levels; on the contrary, aequorin measurements show a strong reduction in cytoplasmic [Ca2+] if Fura-2 is added compared with vehicle.

Major disadvantages of using aequorin

Low light emission by the photoprotein.

In contrast to fluorescent dyes (where up to 104 photons can be emitted by a single molecule before photobleaching occurs), only one photon can be emitted by an aequorin molecule. This means that only a small fraction of the total aequorin pool emits its photon every second: out of the 104–105 molecules per cell of a typical aequorin transfection, light emission will vary from 0 to 1,000 photons at most.

Major disadvantages of using aequorin

Overestimation of the average rise in cells (or compartments) with inhomogeneous behavior.

Because of the steep Ca2+ response curve of aequorin, if the probe is distributed between a high-Ca2+ and a low-Ca2+ domain, the former will undergo a much larger discharge. The total signal will be calibrated as ‘average’ [Ca2+] increase, which will be severely biased by the region with high Ca2+.

Major disadvantages of using aequorin

Cells must be amenable to transfection.

The obvious requirement of this approach is that the cell type being studied must be amenable to transfection.

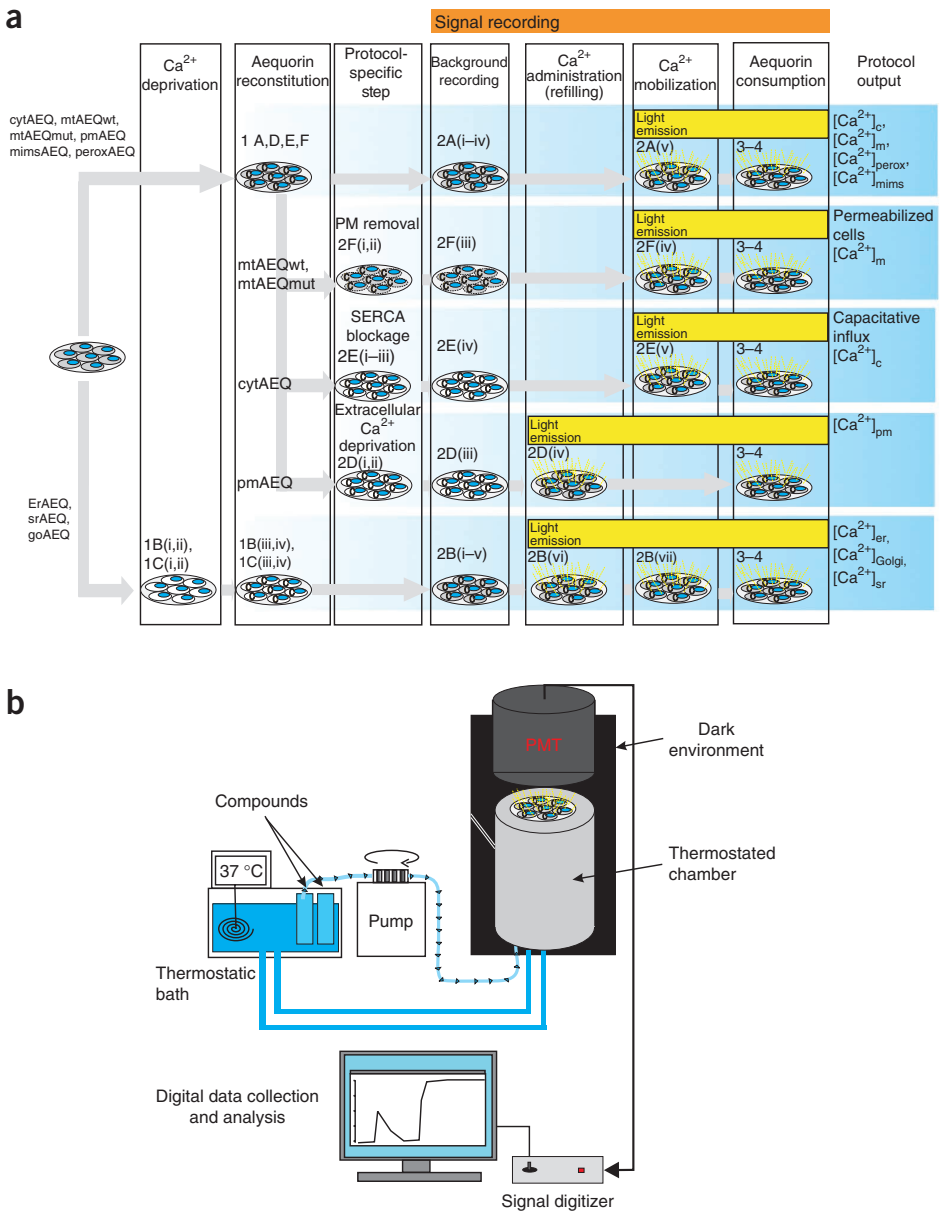

Bonora M. et al., 2013 *Nature Protocols*

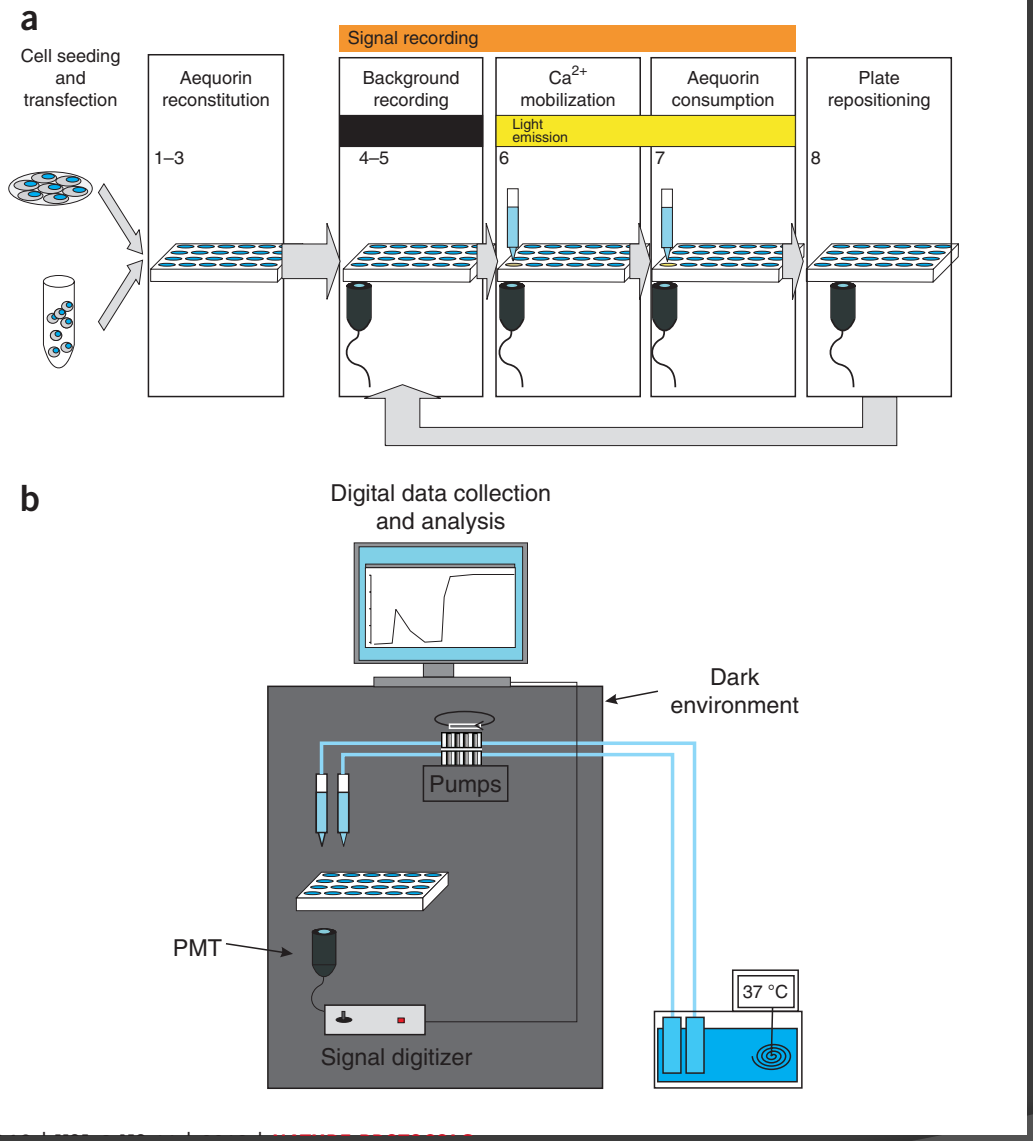

Possibility to perform the experiment on automated plate reader luminometers, which allows for measurements of suspended cells, also in **high-throughput assays**.

Plate-reader luminometers display a reduced sensitivity when compared with single-tube photomultipliers, especially when 96-well plates are used

Bonora M. et al., 2013 *Nature Protocols*

Appropriate controls

A **positive control** for probe expression is provided by cell lysis, which is done as the final phase of each procedure. Light emission induced upon cell lysis is directly proportional to the whole amount of aequorin expression.

A useful **negative control** is to perform the preferred reconstitution and recording procedure in non transfected cells

Genetically encoded Ca2+ indicators (GECI)

intracellular Ca^{2+} detection.

Probe	Origin	Detection technique	Ref.
Aequorin	Genetically encoded	Luminometry	15
Berovin	Genetically encoded	Luminometry	22
Obelin	Genetically encoded	Luminometry	23
Cameleon	Genetically encoded	FRET microscopy	24
Troponin C biosensor	Genetically encoded	FRET microscopy	25
Camgaroo	Genetically encoded	Fluorescence microscopy	26
Ratiometric Pericam	Genetically encoded	Ratiometric fluorescence microscopy	27
GEM-GECO1	Genetically encoded	Ratiometric fluorescence microscopy	28
Calcium Green-1	Synthetic	Fluorescence microscopy	29
Fluo-3, Fluo-4	Synthetic	Fluorescence microscopy	29
Fura-2, Indo-1	Synthetic	Ratiometric fluorescence microscopy	30

FRET-tandem probes modified to measure Ca2+

Bonora M. et al., 2013 *Nature Proocols*

Camaleons

Cameleons are chimeric proteins consisting of a blue or cyan mutant of green fluorescent protein (GFP), calmodulin (CaM), a glycylglycine linker, the CaM-binding domain of myosin light chain kinase (M13), and a green or yellow version of GFP.
Ca2+ binding to the CaM causes intramolecular CaM binding to M13.
The resulting change from an extended to a more compact conformation increases the efficiency of fluorescence resonance energy transfer between the shorter to the longer wavelength mutant GFP.

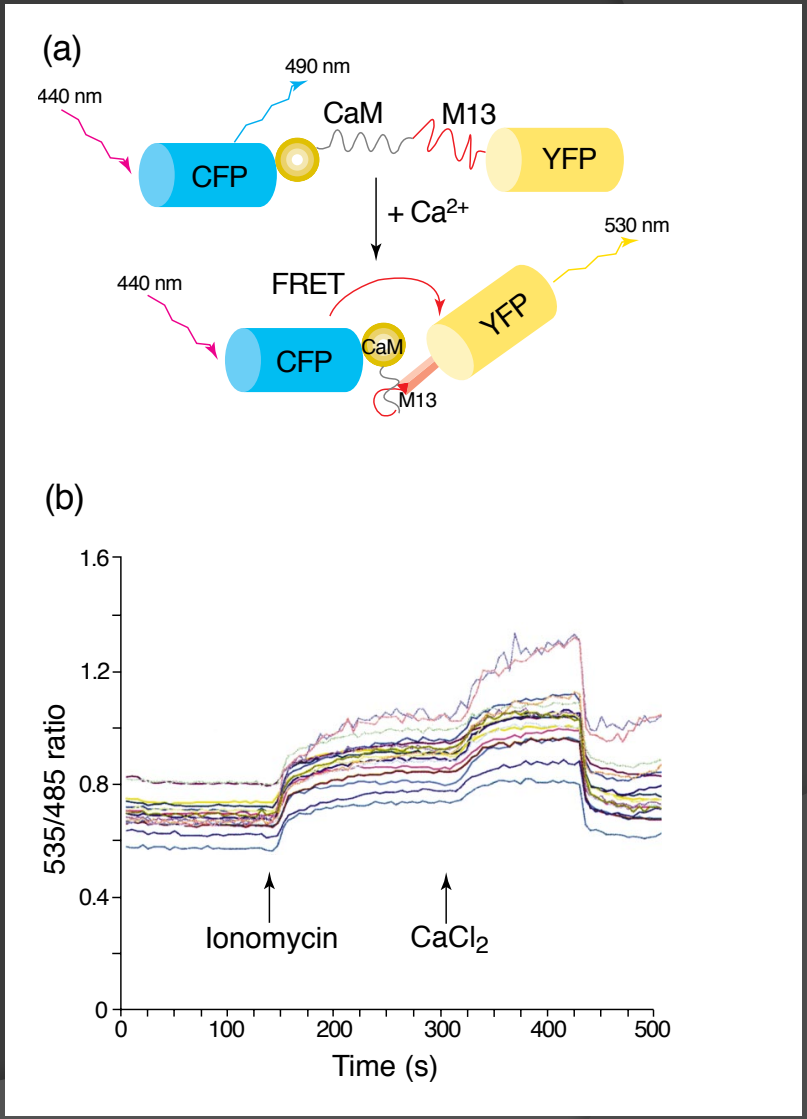

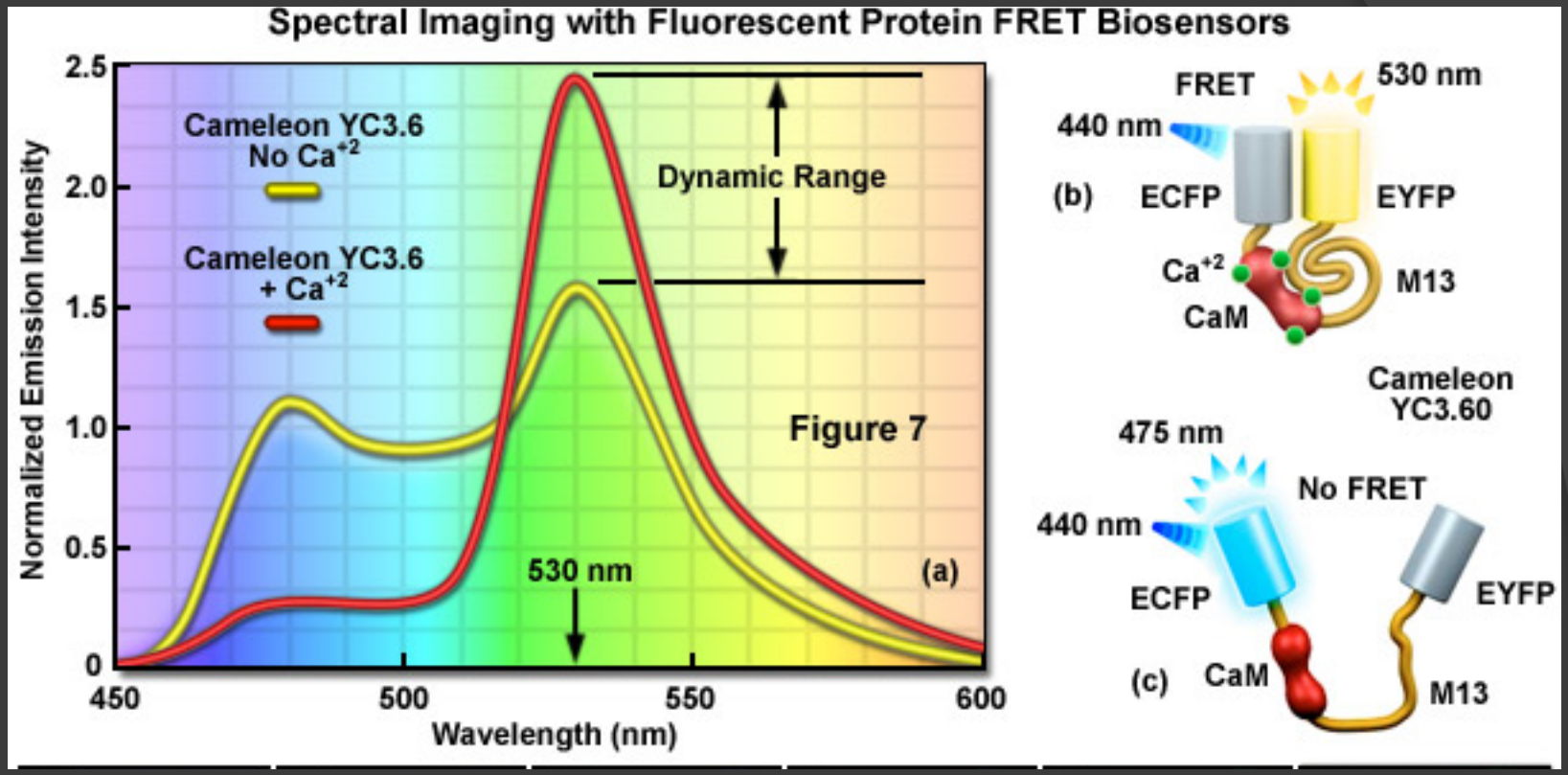

http://zeiss.magnet.fsu.edu/tutorials/spectralimaging/spectralfret/indexflash.html

Camaleons

Because GFP fusions can be expressed *in situ*, they can be targeted to subcellular organelles such as the endoplasmic reticulum (ER), where there are Ca2+ stores. By adjusting the Ca2+ affinities through mutation of the calmodulin protein and establishing that the emission ratio correlated with Ca2+ concentration, the authors measured the free [Ca2+] in both the cytoplasm and ER. They found that the free [Ca2+] in the ER was 60–400 mM in unstimulated cells, falling to 1–50 mM in cells treated with Ca2+ ionophores (e.g. ionomycin).

Genetically encoded Ca2+ indicators (GECI)

- GCaMP

GCaMP

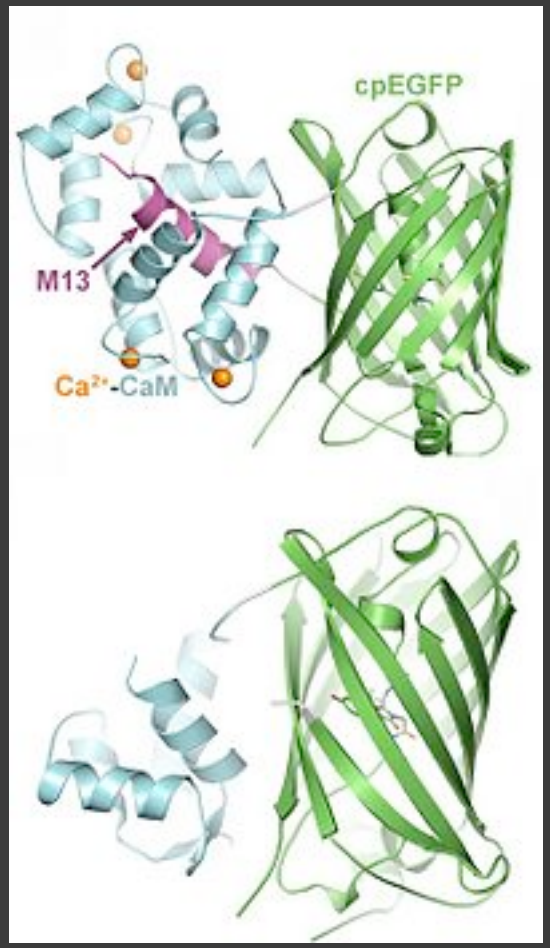

- GCaMP is a genetically encoded, high-affinity Ca2+ sensor that exhibits large fluorescent shifts in response to physiological Ca2+ changes. The sensor comprises a circularly permuted EGFP (cqGFP) flanked by CaM and a CaM-binding peptide (M13) from myosin light chain kinase. Increases in Ca2+ promote Ca2+-CaM-M13 interaction and a conformational change within the sensor, resulting in an increase in EGFP fluorescence

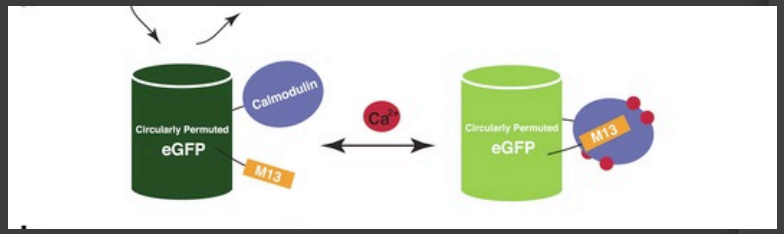

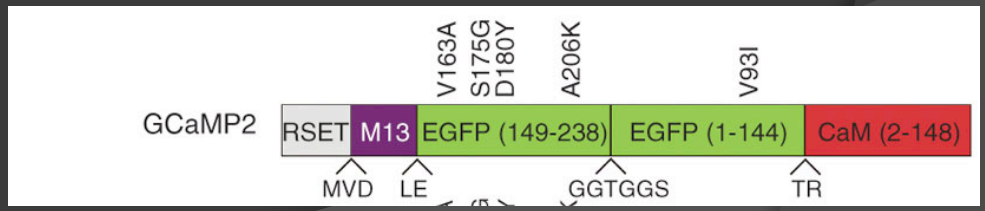

Willoughby, D. et al. J Cell Sci 2010;123:107-117

None of these protein-based indicators have yet surpassed the sensitivity and speed of commonly used synthetic calcium indicators (for example, Oregon Green Bapta-1-AM,OGB1-AM).

Therefore, depending on the experimental goals, investigators choose between sensitive synthetic indicators delivered by invasive chemical or physical methods, or less sensitive protein sensors delivered by genetic methods.

This is of particular interest mainly in neurons.

Because neurons have unusually fast calcium dynamics and low peak calcium accumulations, sensors designed to probe neuronal function are best tested in neurons rather than in non-neuronal systems, most of which show much slower and larger calcium changes.

Make sense therefore to screen GCaMP variants produced by mutagenesis in neurons, and subsequently validated lead sensors in several in vivo systems.

Ultrasensitive fluorescent proteins for imaging neuronal activity

Tsai-Wen Chen[1], Trevor J. Wardill[1]†, Yi Sun[1], Stefan R. Pulver[1], Sabine L. Renninger[2], Amy Baohan[1,3], Eric R. Schreiter[1], Rex A. Kerr[1], Michael B. Orger[2], Vivek Jayaraman[1], Loren L. Looger[1], Karel Svoboda[1] & Douglas S. Kim[1]

18 JULY 2013 | VOL 499 | NATURE | 295

Despite extensive structure-guided optimization GCaMP and other protein sensors still suffer from low sensitivity and slow kinetics.

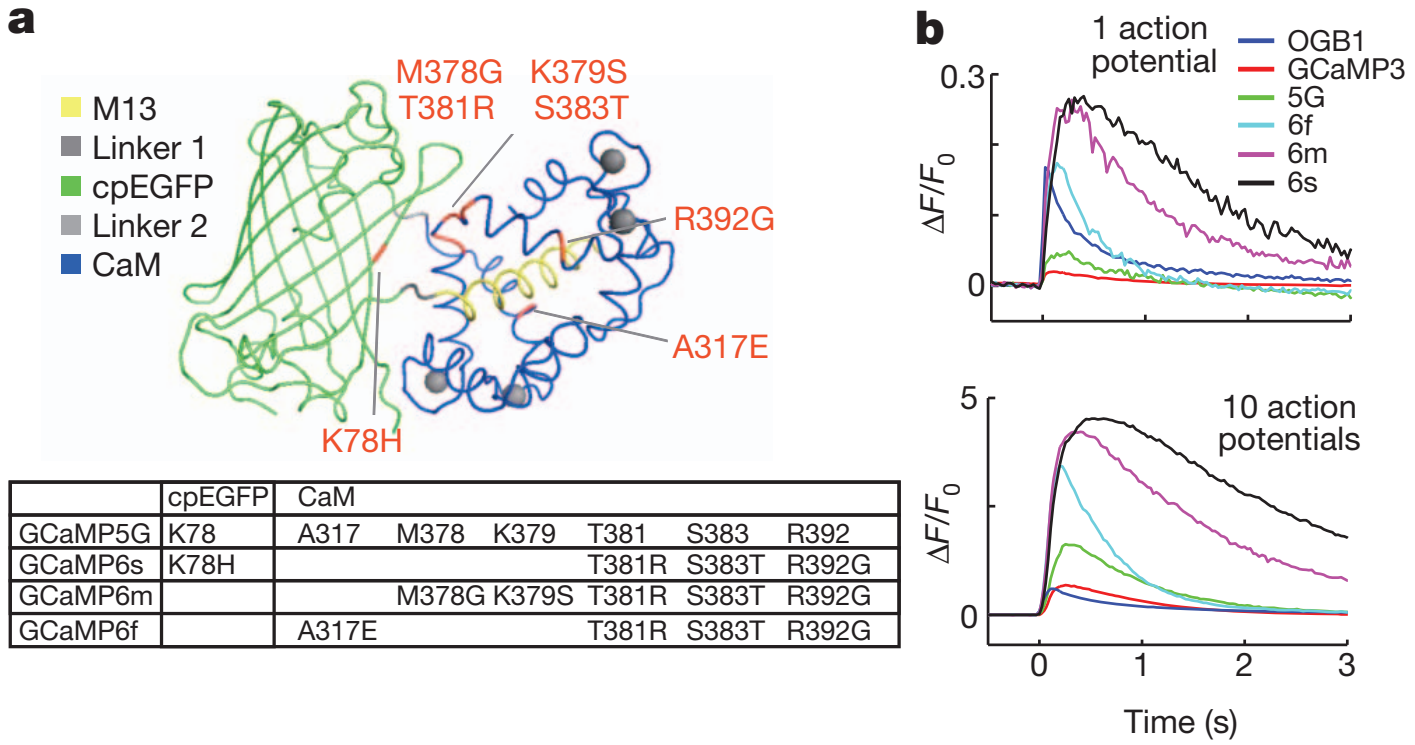

	cpEGFP	CaM					
GCaMP5G	K78	A317	M378	K379	T381	S383	R392
GCaMP6s	K78H				T381R	S383T	R392G
GCaMP6m			M378G	K379S	T381R	S383T	R392G
GCaMP6f		A317E			T381R	S383T	R392G

We produced numerous additional GCaMP variants and tested them in automated neuronal assays (Fig. 1). With the aim of improving sensitivity, we focused mutagenesis on the interface between cpGFP and CaM at 16 amino acid positions, some mutagenized to near completion (Fig. 1a).

Mutations were made at 18 additional sites, notably at the M13–CaM interface which can affect calcium affinity (A317) and in CaM (R392) (Fig. 1a).

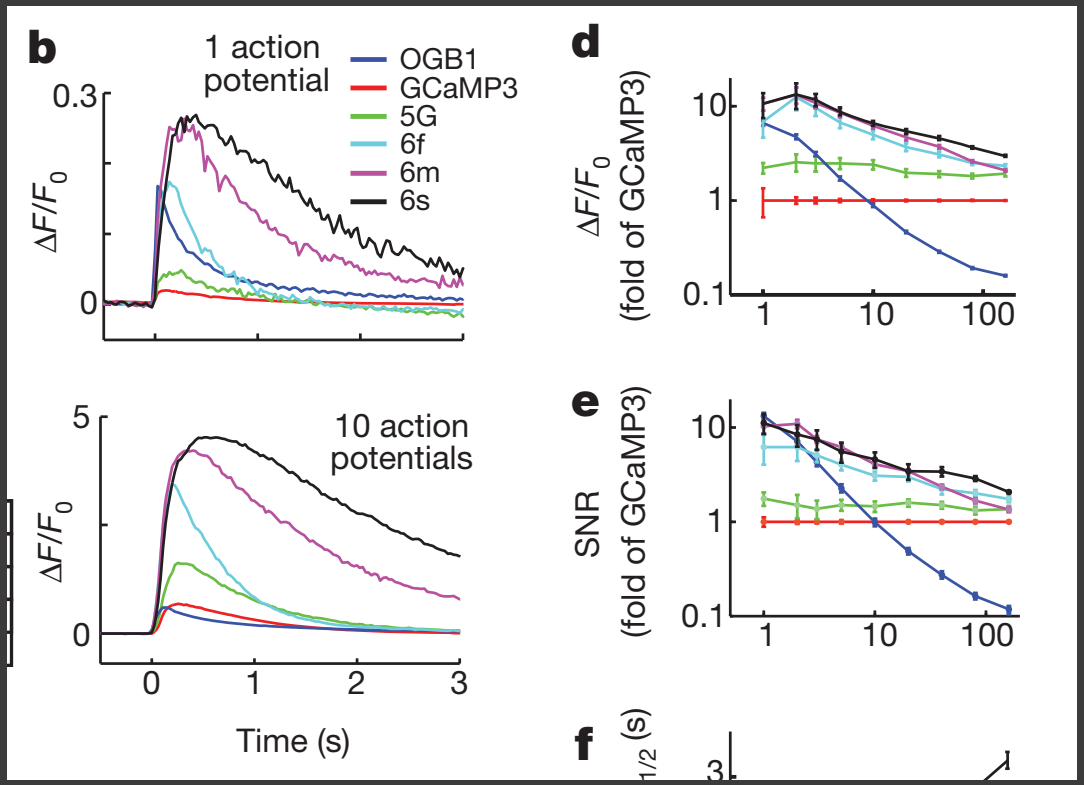

Dissociated rat hippocampal neurons in 24-well plates were transduced with GCaMP variants (one per well), together with nuclear mCherry, using lentivirus-mediated gene transfer. Electrodes triggered trains of action potentials in all neurons within each well.

Time-lapse images (35Hz) of 800 mm fields of view containing 10–100 neurons were acquired, while delivering a series of action potential trains (Fig. 1b).

Fluorescence changes extracted from single neurons were used to compare the sensitivity, dynamic range and kinetics of individual GCaMP variants and OGB1-AM (Fig. 1b–g). We monitored the resting brightness of the sensor by measuring green fluorescence relative to red mCherry fluorescence.

In total, we screened 447 GCaMP variants (Supplementary Table 5).

Based on screening in cultured neurons (Fig. 1), **we chose three ultrasensitive GCaMP6 sensors (GCaMP6s, 6m, 6f; for slow, medium and fast kinetics, respectively) for characterization in vivo.**

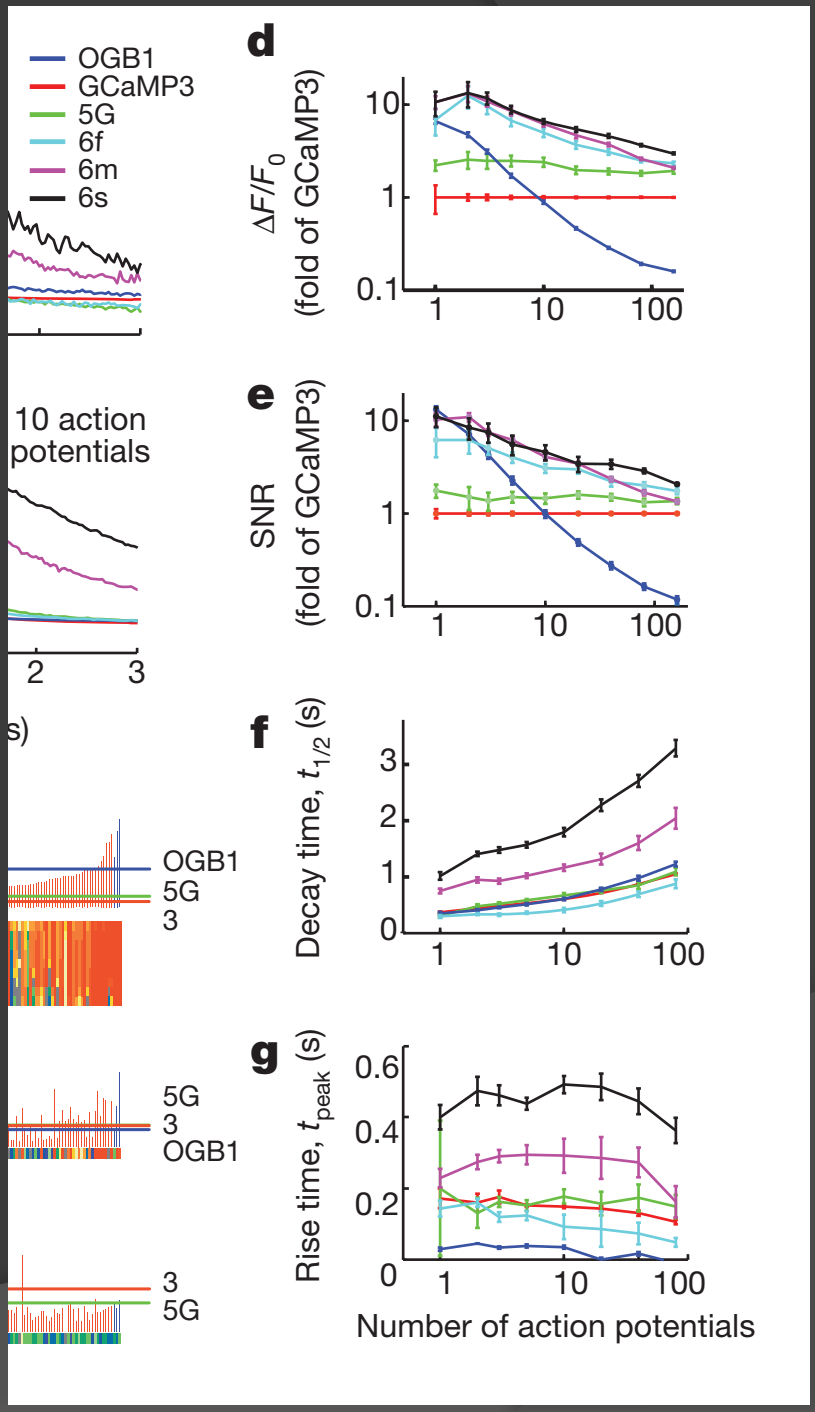

Compared to GCaMP5G, the GCaMP6 sensors have similar baseline brightness and a 1.1- to 1.6-fold increase in dynamic range (DF/F0 at 160 action potentials).

For small numbers of action potentials the most sensitive sensor, GCaMP6s, produced sevenfold larger signals (.10-fold larger than GCaMP3, Fig. 1b–e). Compared to GCaMP5G, GCaMP6s exhibited threefold higher apparent affinity for calcium and 1.3-fold higher saturated fluorescence, with similar baseline fluorescence. Calcium saturated GCaMP6s is 27% brighter than enhanced GFP (EGFP), its parent fluorescent protein.

The fastest sensor, **GCaMP6f**, had two fold faster rise time and 1.7-fold faster decay time thanGCaMP5G(Fig. 1f, g). **GCaMP6f is the fastest genetically-encoded calcium indicator for cytoplasmic free calcium in neurons, with sensitivity comparable to OGB1-AM**(Fig. 1d–g).

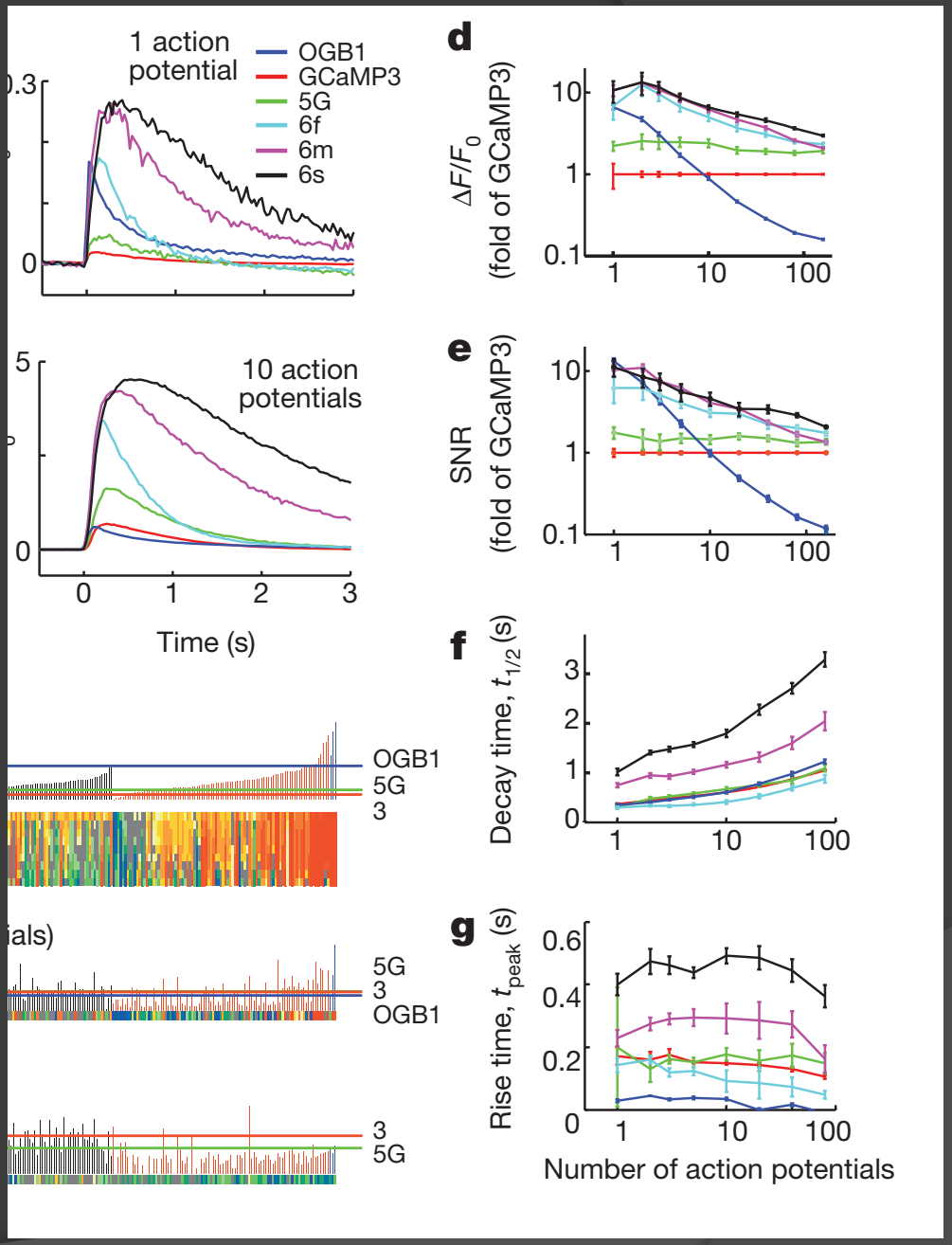

GCaMP6 performance in the mouse visual cortex.

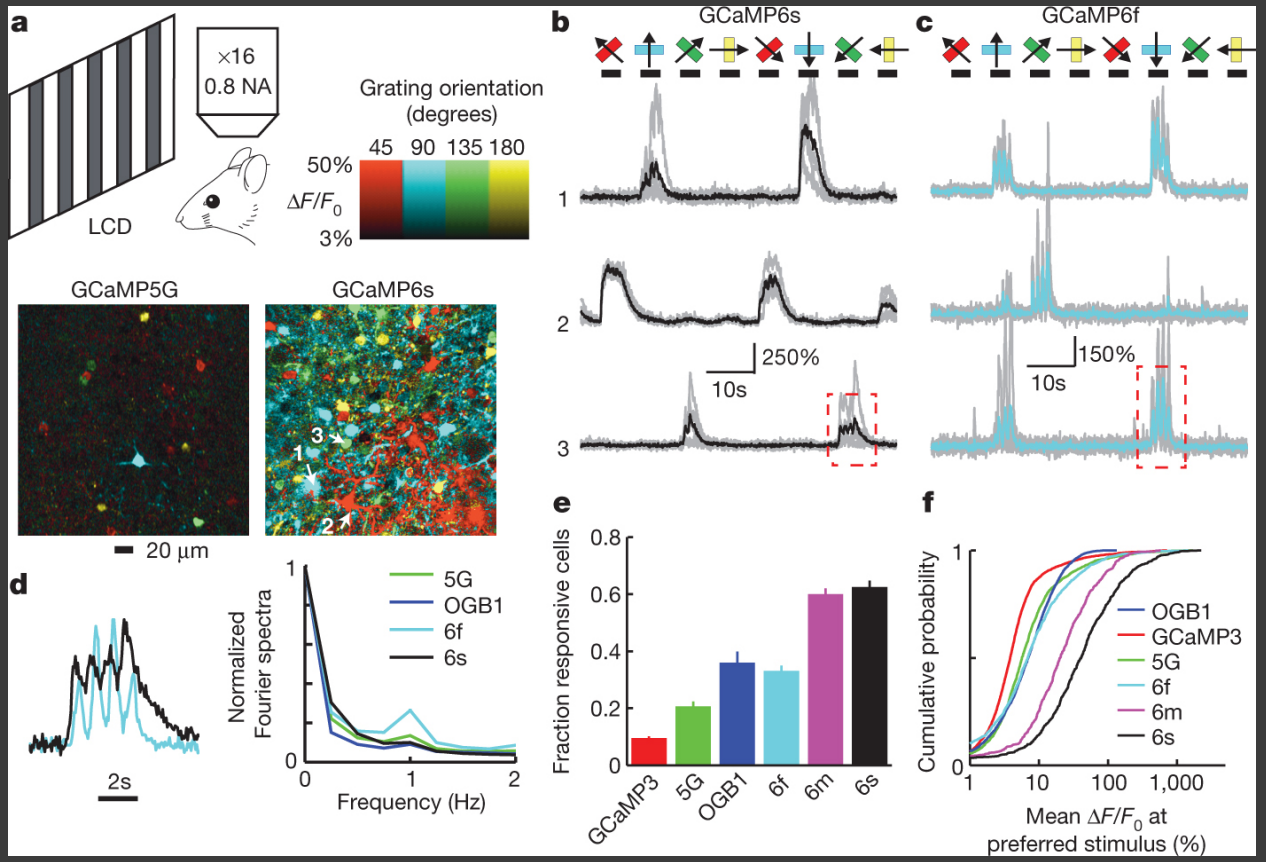

We next tested GCaMP6 in layer (L) 2/3 pyramidal neurons in the mouse visual cortex V1 in vivo. V1 was infected with adeno-associated virus (AAV) expressing GCaMP variants (AAV-hsyn1-GCaMP variant). Three weeks afterAAV infection, the vast majority of L2/3 neurons showed fluorescence mainly in the neuronal cytoplasm

GCaMP6 performance in the mouse visual cortex.

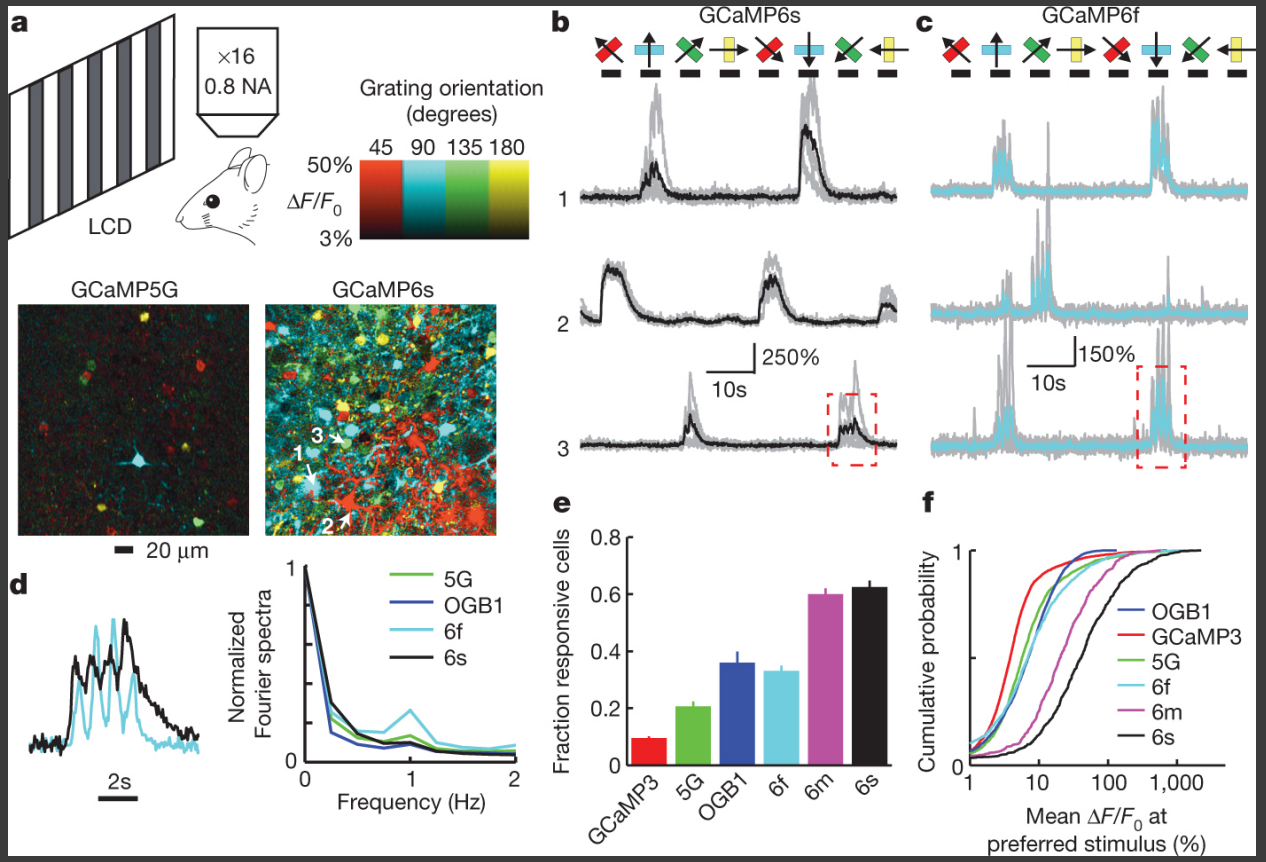

Sensory stimuli consisted of moving gratings presented in eight directions to the contralateral eye. Two-photon imaging revealed visual stimulus-evoked fluorescence transients in subsets of neurons (Fig. 2a–c). Fluorescence transients were faster with GCaMP6f compared to other sensors and faithfully tracked dynamic sensory stimuli (Fig. 2d).

GCaMP6 performance in the mouse visual cortex.

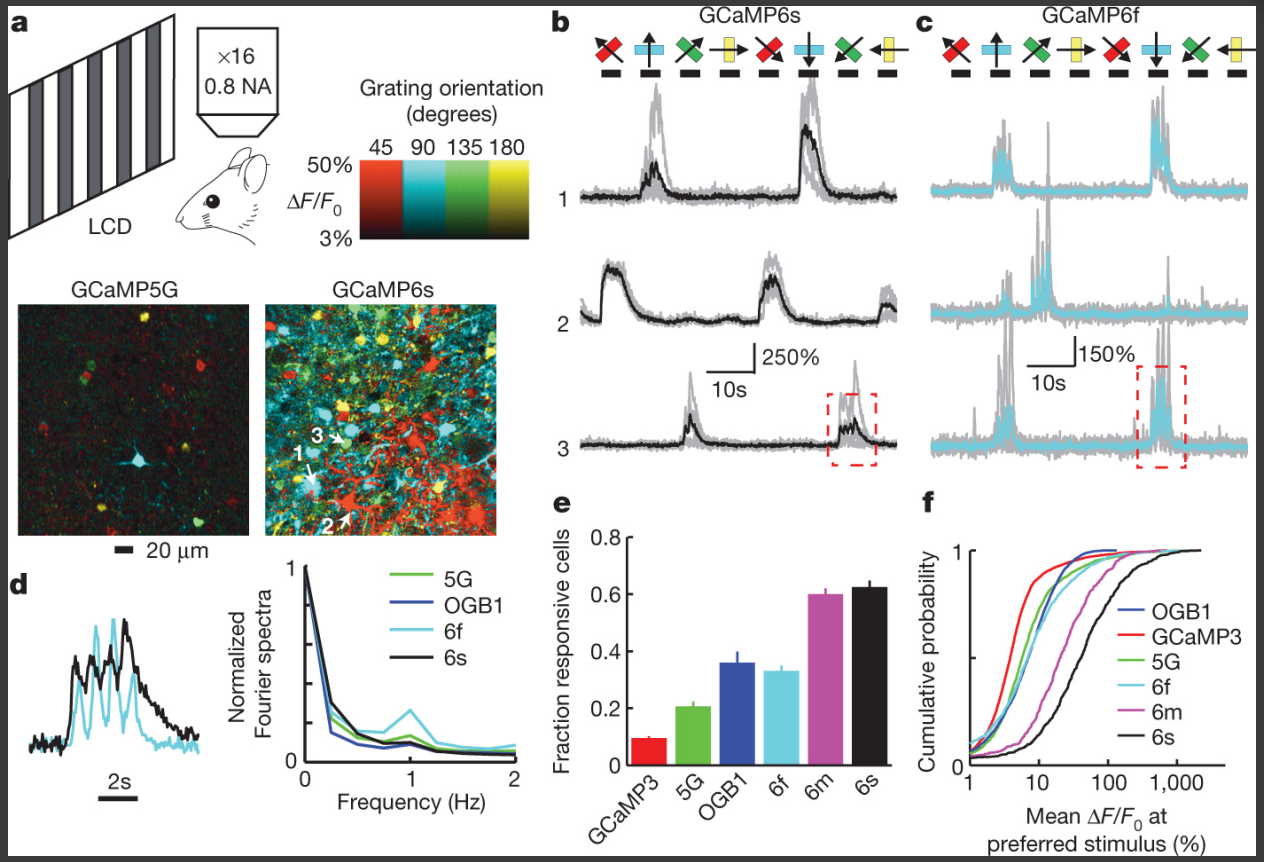

GCaMP6 performance was compared to other sensors in several ways. The fraction of responding neurons detected with GCaMP6s was threefold higher than for GCaMP5G (fivefold higher than GCaMP3) (Fig. 2e). Notably, the fractions of active neurons detected with GCaMP6s and GCaMP6m were also significantly higher than for OGB1-AM (Fig. 2e, f, P,0.01, Wilcoxon rank sum test). GCaMP6 sensors thus reveal neuronal dynamics that were previously undetectable with protein sensors.

GCaMP6 performance in the mouse visual cortex.

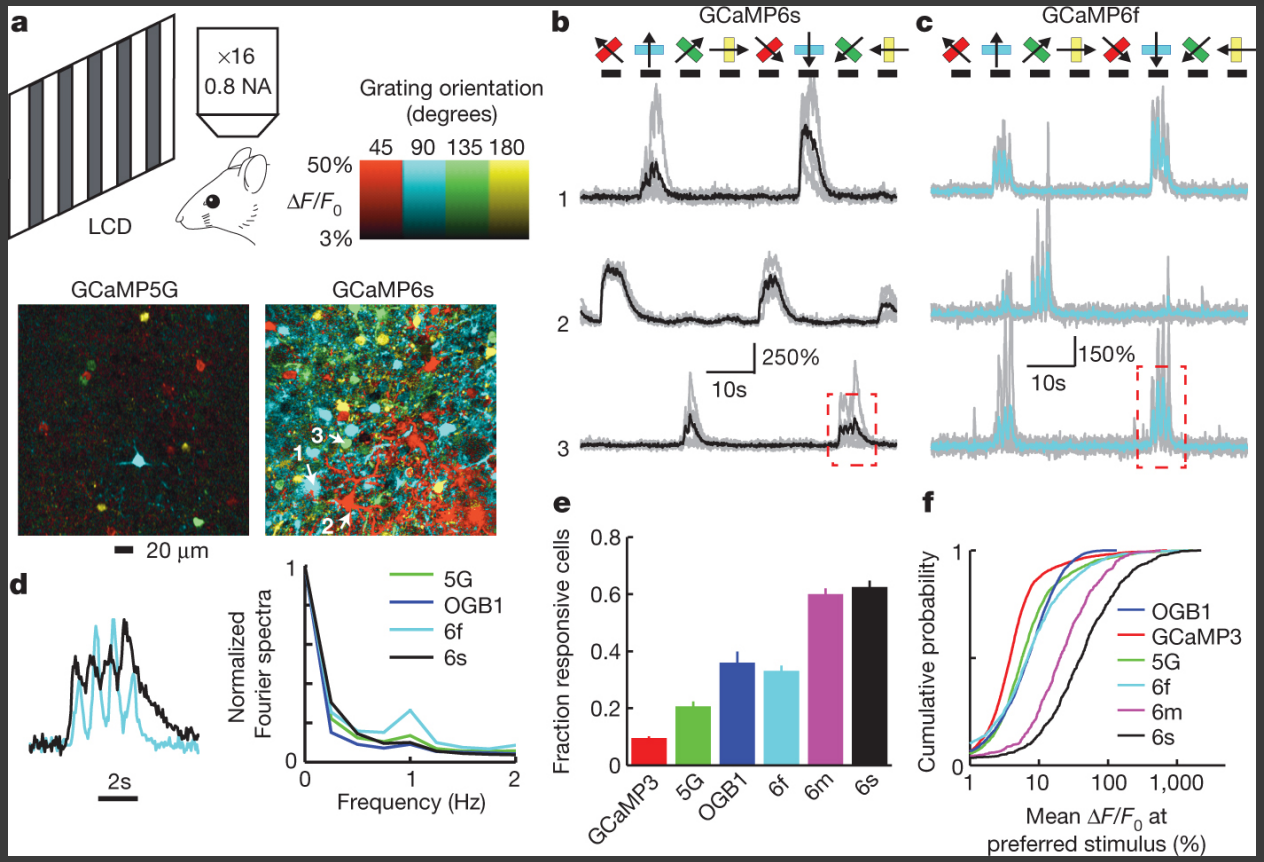

GCaMP6 sensors thus reveal neuronal dynamics that were previously undetectable with protein sensors.

Combined imaging and electrophysiology in the visual cortex.

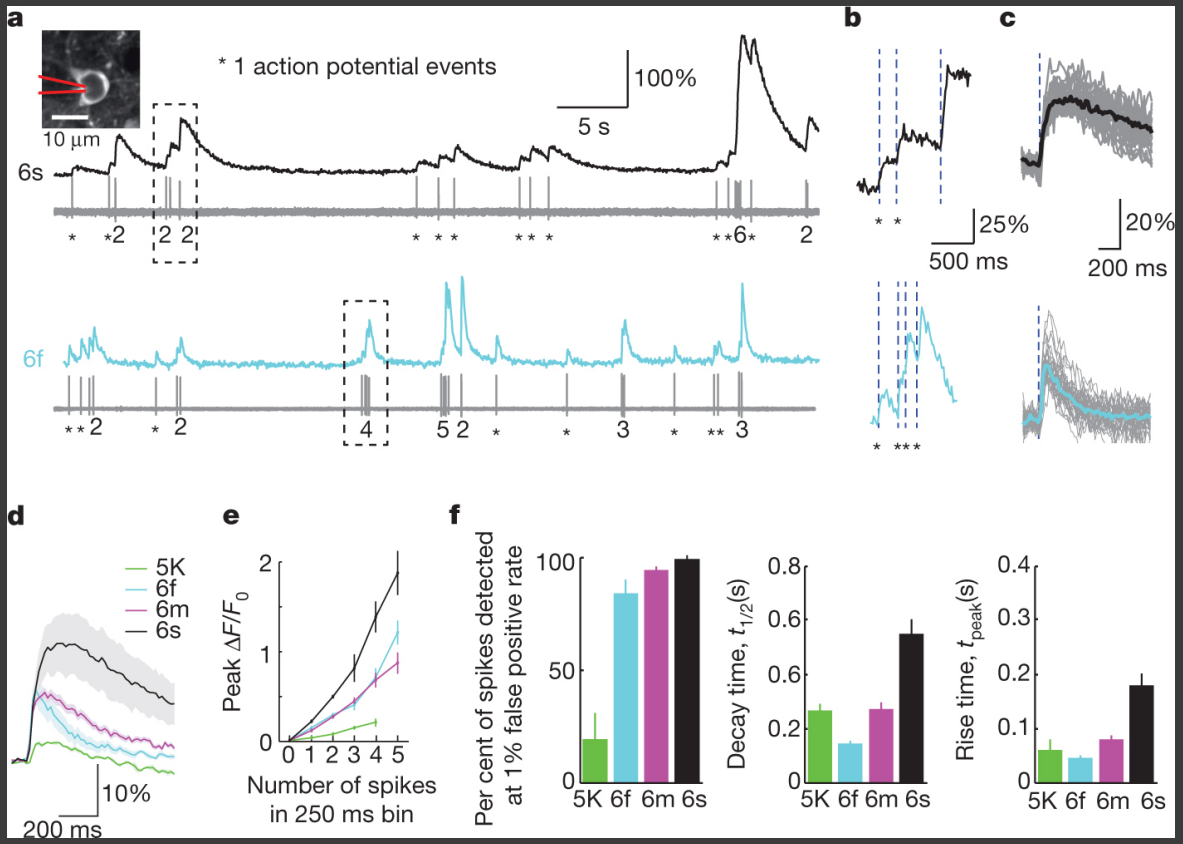

We directly compared cellular fluorescence changes and spiking using loose-seal, cell-attached recordings. GCaMP6s produced large fluorescence transients even in response to single action potentials (.6 times larger than for GCaMP5K, Fig. 3 and Supplementary Video 1), yielding high detection rates for single spikes.


20%
0.5mV
1s
10 µm

Combined imaging and electrophysiology in the visual cortex.

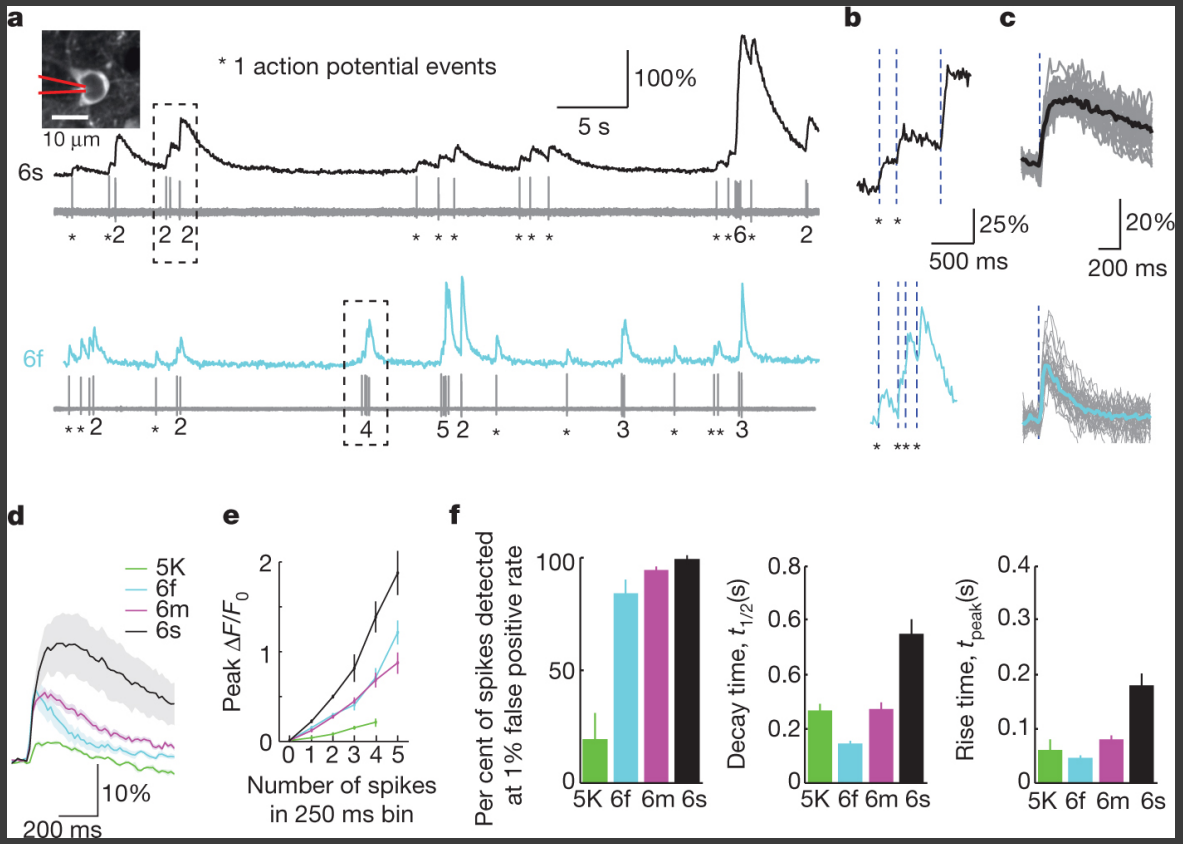

GCaMP6f and GCaMP6m showed slightly lower spike detection efficiencies, but with faster kinetics (Fig. 3). Individual spikes within a burst resulted in stepwise fluorescence increases (Fig. 3b), which were resolvable if they were separated by an interval on the order of the rise time of the sensor or more (100–150ms, GCaMP6s; 75–100 ms, GCaMP6m; 50–75ms, GCaMP6f).

GCaMP6 indicators cross important performance thresholds. They have higher sensitivity than commonly used synthetic calcium dyes (for example, OGB1-AM) and detect individual action potentials with high reliability at reasonable microscope magnifications. These indicators can be used to image large groups of neurons as well as tiny synaptic compartments over multiple imaging sessions separated by months. It is likely that these sensors will find widespread applications for diverse problems in brain research and calcium signalling.

Neuron
NeuroResource

Imaging Neural Activity Using *Thy1*-GCaMP Transgenic Mice

Qian Chen,[1] Joseph Cichon,[3,10] Wenting Wang,[1,10] Li Qiu,[4] Seok-Jin R. Lee,[4] Nolan R. Campbell,[1] Nicholas DeStefino,[6] Michael J. Goard,[2] Zhanyan Fu,[1,5] Ryohei Yasuda,[4] Loren L. Looger,[7] Benjamin R. Arenkiel,[8] Wen-Biao Gan,[3] and Guoping Feng[1,9,*]

[1]McGovern Institute for Brain Research, Department of Brain and Cognitive Sciences
[2]Picower Institute for Learning and Memory, Department of Brain and Cognitive Sciences
Massachusetts Institute of Technology, Cambridge, MA 02139, USA
[3]Molecular Neurobiology Program, Skirball Institute, Department of Physiology and Neuroscience, New York University School of Medicine, New York, NY 10016, USA
[4]Department of Neurobiology
[5]Department of Psychiatry and Behavioral Science
Duke University Medical Center, Durham, NC 27710, USA
[6]MD-PhD Program, Harvard Medical School, Boston, MA 02115, USA
[7]Howard Hughes Medical Institute, Janelia Farm Research Campus, Ashburn, VA 20147, USA
[8]Department of Molecular and Human Genetics, Baylor College of Medicine, Houston, TX 77030, USA
[9]Stanley Center for Psychiatric Research, Broad Institute, Cambridge, MA 02142, USA
[10]These authors contributed equally to this work
*Correspondence: fengg@mit.edu
http://dx.doi.org/10.1016/j.neuron.2012.07.011